Available online at www.sciencedirect.com
SCIENCE DIRECT®
Biochemical and Biophysical Research Communications 313 (2004) 496–502
BBRC
www.elsevier.com/locate/ybbrc

Tyrosine-728 and glutamic acid-735 are essential for the metalloproteolytic activity of the lethal factor of *Bacillus anthracis*

Fiorella Tonello,[a,*] Laura Naletto,[b] Vanina Romanello,[b] Federica Dal Molin,[b] and Cesare Montecucco[b]

[a] *Istituto di Neuroscienze del CNR, Università di Padova, Via G. Colombo 3, 35121 Padua, Italy*
[b] *Dipartimento di Scienze Biomediche, Università di Padova, Via G. Colombo 3, 35121 Padua, Italy*

Received 19 November 2003

Abstract

The lethal factor (LF) of *Bacillus anthracis* is a Zn^{2+}-endopeptidase specific for the MAPK-kinase family of proteins. The catalytic zinc atom is coordinated by a first shell of residues including the two histidines and the glutamate of the zinc-binding motif HExxH and by Glu-735. A characteristic feature of LF is the presence, within the second shell of residues, of a tyrosine (Tyr-728) in close proximity (3.3 Å) to the zinc atom. To investigate the role of Tyr-728 and Glu-735, LF mutants with one or both of these two residues replaced by Ala were cloned, expressed, and purified from *Escherichia coli*. A fourth mutant was obtained by replacing Tyr-728 with Phe. Spectroscopic analysis of these mutants indicates that they fold in the same way as the parental molecule and that zinc stabilizes the structure of LF. These mutants have neither proteolytic activity nor in vivo toxicity. The possible role of Tyr-728 in catalysis is discussed.

Keywords: Anthrax lethal factor; Metalloprotease active site; Site-directed mutagenesis; Zinc coordination; Mitogen-activated protein kinase kinase; Peptide substrate; Macrophage; Fischer rat; Action mechanism

Anthrax lethal factor (90.2 kDa, LF) is secreted by toxigenic strains of *Bacillus anthracis* together with protective antigen (87.2 kDa, PA) and edema factor (88.8 kDa, EF) [1,2]. PA binds to a plasma membrane ubiquitous receptor (ATR: anthrax toxin receptor) which is a type I membrane protein [3], and it is then proteolytically processed by membrane furin-like peptidases including furin to a 63 kDa form which oligomerizes and binds LF [2]. Following endocytosis, PA undergoes a low pH-triggered conformational rearrangement [4], that mediates the transfer of LF from the lumen of a late endocytic compartment to the cytoplasm [5]. Within the cytosol, LF displays its metalloproteolytic activity directed toward the N-terminus of the MAPK-kinase family of proteins [6–8]. The consensus motif of residues recognized by LF is a cluster of positively charged residues followed by an aliphatic hydrophobic residue in position P1 [8,9]. LF + PA is cytotoxic to macrophages [10] where it induces the production of reactive oxygen intermediates [11]. LF + PA also induces cell death by apoptosis in macrophages stimulated by lipopolysaccharide (LPS) [12]. There is evidence that LF + PA action on macrophages plays a major role in the development of systemic anthrax, a rapid and often fatal disease of several vertebrate species including humans (see Dixon et al. for a recent review [13]).

LF is a 90 kDa protein containing a C-terminal HExxH Zn^{2+}-binding site (amino acids 686–690 of mature LF) present in the active site of metallopeptidases [14]. LeTx cytotoxicity depends on LF proteolytic activity, as membrane permeable metalloprotease inhibitors prevent its cytotoxic activity on cultured macrophages [15]. The crystallographic structure of LF shows the presence of four domains [16]. The N-terminal domain (residues 27–262) is responsible for binding to PA. The region comprising residues 263–550 has a defined homology with the *Bacillus cereus* ADP-ribosyltransferase insecticidal protein toxin VIP2. It includes the region 300–386 which protrudes out of the domain

* Corresponding author. Fax: +39-049-827-6049.
E-mail address: fiorella.tonello@unipd.it (F. Tonello).

0006-291X/$ - see front matter © 2003 Elsevier Inc. All rights reserved.
doi:10.1016/j.bbrc.2003.11.134

and shapes the boundary of the cleft-shaped active site of LF; a role in substrate recognition is suggested by the fact that a deletion of part of it renders LF inactive [17]. The fourth domain is formed by segment 551–777 and consists of a metalloprotease with a classical zinc-binding motif His^{686}–Glu^{687}–X– X–His^{690} [14,15,18]. Mutation of the active site residues which form the first shell of residues around the metal atom partially or totally impairs LF activity [14,19]. The zinc atom is coordinated by an additional glutamate located further down in the sequence (Glu-735). Such zinc coordination resembles that of the thermolysin family of metalloproteases, but an analysis of the second shell of residues surrounding the zinc atom reveals the presence of a tyrosine residue (Tyr-728) absent in thermolysin. A similar tyrosine is instead present in the clostridial metalloprotease neurotoxins which comprises eight members: seven botulinum neurotoxins and one tetanus neurotoxin [20,21]. Mutation of this tyrosine of tetanus neurotoxin (Tyr-375) and in botulinum neurotoxin type A (Tyr-366) into an alanine impairs their proteolytic activity, suggesting that the phenolic side chain plays a role in catalysis and/or in substrate binding [22,23].

We have extended these studies to LF and here we describe the properties of such tyrosine mutants in comparison with mutants of Glu-735 which is directly involved in zinc coordination. We also describe the preparation and properties of the double mutant $LF^{Y728A;E735A}$ which could be considered for vaccine studies where a totally inactive non-reversible LF mutant is required.

Materials and methods

Chemicals. Thrombin, GSH–Sepharose 4B, and benzamidine resin were purchased from Amersham Pharmacia Biotech. All chemicals and reagents were purchased from Sigma or Fluka.

Site-directed mutagenesis. LF wild type gene was sub-cloned from pGEX-2Tk LF [7] in *Bam*HI site of pGEM-3Zf (Promega). PGEM-3Zf-LF was used as template in a PCR amplification performed using the Quickchange site-directed mutagenesis kit (Stratagene). The primers employed were: CGCTTCATTTGTTCTCCCAGCCGAAG TTAAATTACTCCC (forward), GGGAGTAATTTAACTTCGGCT GGGAGAACAAATGAAGCG (reverse) for the mutation Y728A; GGGAGTAATTTAACTTCGTTTGGGAGAACAAATGAAGCG (forward), CGCTTCATTTGTTCTCCCAAACGAAGTTAAATTAC TCCC (reverse) for the mutation Y728F; and CTAAAGGCTTCTGC AAAAAATGCCGCTTCCTTTGTTCTCCC (forward), GGGAGAA CAAATGAAGCGGCATTTTTTGCAGAAGCCTTTAG (reverse) for the mutation E735A. PCR was performed under the following conditions: initial denaturation for 30 s at 95 °C, 16 cycles of 30 s at 95 °C, 1 min at 55 °C, and 10.5 min at 68 °C. After digestion of the parental DNA for 1 h at 37 °C with *Dpn*I, the amplified plasmids were transformed into *Escherichia coli* XL-1 Blue competent cells. The presence of the mutation was confirmed by DNA sequencing. Finally the LF mutant genes were sub-cloned in *Bam*HI site of pGEX-2Tk.

Protein expression and purification. MKK3 (mitogen-activated protein kinase kinase 3), LF [7], and LF mutants were expressed as glutathione *S*-transferase (GST) fusion proteins in *E. coli* BL21 (DE3) pUBS and purified as previously described [7]. The PA gene from the plasmid pACP71 [24] was PCR amplified using the following primers: GGAATTCCATATGGAAGTTAAACAGGAGAACCGG (forward) and AGACTCGAGTTATCCTATCTCATAGCCTTTTTT (reverse). The PCR fragment obtained was digested with *Nde*I and *Xho*I and inserted in the vector pET19 (Novagen). The inserted sequence was confirmed by DNA sequencing. The protein was expressed as N-terminal His-tag fusion protein in BL21 (DE3) (Novagen) and purified by HiTrap chelating (Pharmacia) charged with Ni ions. Protein activity was tested in Raw267.4 cells resulting in being identical to that of native PA purified from *Bacillus anthrax* [7].

Protein concentration determination. Protein concentration was determined by measuring the absorbance at 280 nm using a Perking–Elmer lambda-6 spectrophotometer. The absorption coefficients at 280 nm and 0.1% (by mass) protein concentration were, respectively, 0.798 mg^{-1} cm^2 for wild type LF, 0.785 mg^{-1} cm^2 for LF^{Y728A} and LF^{Y728F}, 0.799 mg^{-1} cm^2 for LF^{E735A} and 0.786 mg^{-1} cm^2 for the double mutant.

Preparation of apo-LF. LF 3 μM was dialysed against a buffer containing 10 mM of 1-10-phenanthroline (OP), 10 mM Tris–HCl, 60 mM NaCl, and 0.5 mM ethylenediaminetetraacetic acid (EDTA), pH 8.0. Successively the protein solution was dialysed against the same buffer without OP, treated with Chelex 20 (Fluka) to eliminate metal ions.

Analysis of zinc content. The zinc content of the mutants and the wild type toxin was measured using a Perkin–Elmer 4000 atomic absorption flame spectrophotometer. After purification of the recombinant protein, metal content of samples containing 3 μM of protein was measured after standardization in the linear range of 0–0.5 ppm of zinc and the buffer was used as blank. Analysis were performed in triplicate.

Circular dichroism spectroscopy. Measurements of optical ellipticity were made at room temperature on a Jasco J-710 spectropolarimeter in a 0.1-cm path-length quartz cell (240–190 nm) or 1 cm path-length quartz cell (350–250 nm) at a protein concentration of 3 μM in 20 mM Tris–HCl, pH 8.0, 100 mM NaCl. Ellipticities were normalized to residue concentration using the relationship $[\theta] = (\theta_{obs}/10) \cdot (M/l \cdot c)$ where θ_{obs} is the observed ellipticity at a given wavelength, M is the mean residue mass, l is the cuvette pathlength in centimeters, and c is the protein concentration expressed as g/ml. All CD spectra resulted from an averaging of at least four scans and the final spectrum was corrected by subtracting the corresponding buffer spectrum obtained under identical conditions.

Protein denaturation. The urea-induced unfolding process of LF wild type, apo-LF, and LF mutants was followed by monitoring the fluorescence emission signal at 340 nm (280 nm excitation wavelength) as a function of increasing urea concentrations. For each data point, LF and mutants were treated at 1 μM final concentration in 20 mM Tris–HCl, 100 mM NaCl, pH 8.0, with the appropriate urea solution. Fluorescence was recorded in a 1-cm path-length quartz cell kept at 25 °C on a Perkin–Elmer LS-50 spectrofluorimeter.

Proteolytic activity. Wild type and mutant LF proteolytic activity was determined both on LF peptide substrates [9] and on GST-MKK3. The release of pNA from Ac(R)8VLRpNA dissolved at a concentration of 5 μM in 25 mM Na_2HPO_4, pH 7.4, 15 mM NaCl was monitored at 405 nm by a spectrophotometer Perkin–Elmer Lambda 6 at 25 °C.

The cleavage of GSH–Sepharose bead-immobilized MKK3 was performed at an enzyme/substrate ratio of 1:20 (w/w) for 2 h at 37 °C in 10 mM Tris, 60 mM NaCl, pH 7.4. The reactions were separated by 12% SDS–PAGE and gel stained with Simply Blue (Invitrogen).

Macrophage cytotoxicity of LF. The RAW264,7 mouse macrophage cell line is commonly used to test LF-induced cytotoxicity. Cells were grown in DMEM supplemented with 10% FCS and antibiotics, and incubated in 5% CO_2 in air at 37 °C. PA (800 ng/ml) and LF wild type and mutants (400 ng/ml) were added to cells seeded 24 h before (2×10^4 per well) in 96-well plate in DMEM supplemented with 10% FCS. Cell viability was determined by CellTiter 96 assay (Promega) after 4 h.

Toxicity on Fischer 344 rats. The rats (weighting around 250 g) were anesthetized using isoflurane. A femoral vein was uncovered and LeTx (12 mg LF or LF^{Y728F} + 30 mg PA) was injected intravenously. The development of symptoms was monitored up to 24 h. Animals were suppressed when acute respiratory distress developed.

Results

Site-specific mutagenesis of the anthrax lethal factor

The structure of LF has revealed that the three residues of the zinc-binding motif and Glu-735 are the four ligands of the catalytic zinc atom [16]. In addition, a secondary layer of residues, less close to the zinc atom, is present at the active site and includes Tyr-728 which is only 3.3 Å away from zinc and points its phenolic ring inside the cleft-shaped active site of the toxin (Fig. 1). On the basis of the previous demonstration of the importance for proteolysis of the corresponding tyrosine in the clostridial neurotoxin metalloproteases (tetanus neurotoxin Tyr-375; botulinum neurotoxin A Tyr-366), Tyr-728 was selected as target for mutagenesis and replaced with Ala or with Phe, using a PCR-based mutagenesis procedure. (Fig. 2). For comparison, we have

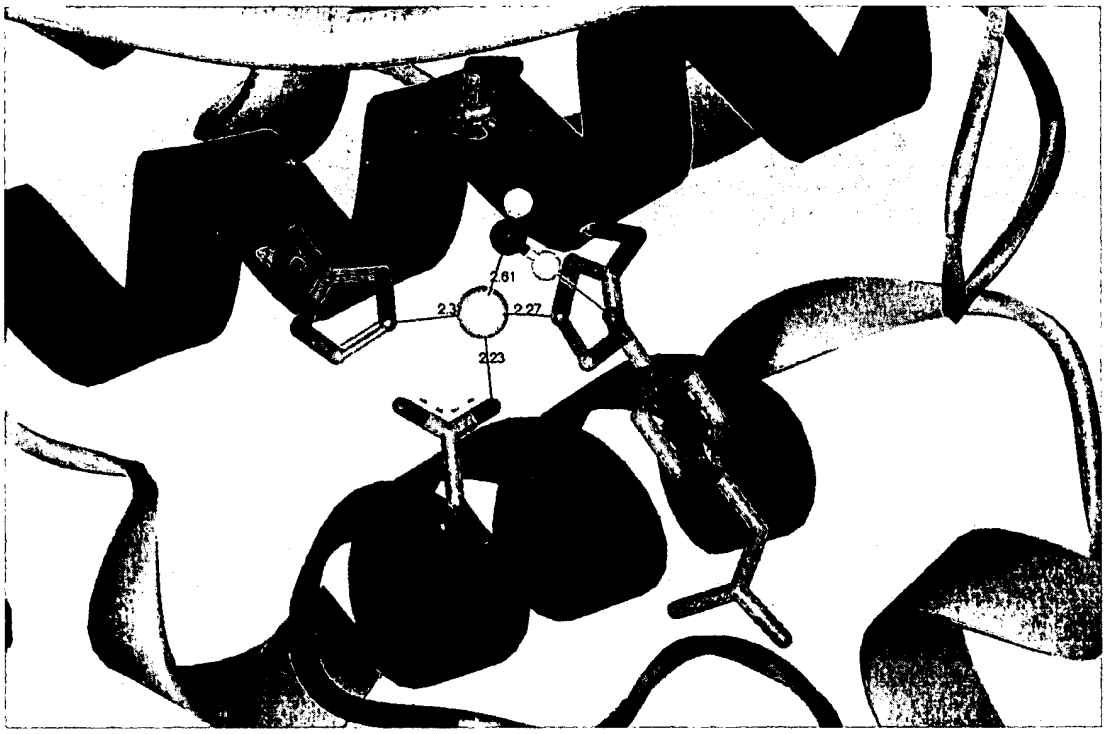


```
  1 AGGHGDVGMH VKEKEKNKDE NKRKDEERNK TQEEHLKEIM KHIVKIEVKG EEAVKKEAAE KLLEKVPSDV
 71 LEMYKAIGGK IYIVDGDITK HISLEALSED KKKIKDIYGK DALLHEHYVY AKEGYEPVLV IQSSEDYVEN
141 TEKALNVYYE IGKILSRDIL SKINQPYQKF LDVLNTIKNA SDSDGQDLLF TNQLKEHPTD FSVEFLEQNS
211 NEVQEVFAKA FAYYIEPQHR DVLQLYAPEA FNYMDKFNEQ EINLSLEELK DQRMLSRYEK WEKIKQHYQH
281 WSDSLSEEGR GLLKKLQIPI EPKKDDIIHS LSQEEKELLK RIQIDSSDFL STEEKEFLKK LQIDIRDSLS
351 EEEKELLNRI QVDSSNPLSE KEKEFLKKLK LDIQPYDINQ RLQDTGGLID SPSINLDVRK QYKRDIQNID
421 ALLHQSIGST LYNKIYLYEN MNINNLTATL GADLVDSTDN TKINRGIFNE FKKNFKYSIS SNYMIVDINE
491 RPALDNERLK WRIQLSPDTR AGYLENGKLI LQRNIGLEIK DVQIIKQSEK EYIRIDAKVV PKSKIDTKIQ
561 EAQLNINQEW NKALGLPKYT KLITFNVHNR YASNIVESAY LILNEWKNNI QSDLIKKVTN YLVDGNGRFV
631 FTDITLPNIA EQYTHQDEIY EQVHSKGLYV PESRSILLHG PSKGVELRND SEGFIHEFGH AVDDYAGYLL
701 DKNQSDLVTN SKKFIDIFKE EGSNLTSYGR TNEAEFFAEA FRLMHSTDHA ERLKVQKNAP TFQFINDQI
771 KFIINS
```

Fig. 1. (Upper panel) Active site of anthrax lethal factor reconstructed using the 3D coordinates (J7NA) deposited in the Protein Data Bank (PDB). Helix 4α2 [16], which contains the HExxH motif, is coloured in blue; helix 4α6, from which Tyr-728 protrudes, is coloured orange while helix 4α7 containing Glu-735 is green coloured. Zinc ion is represented by a yellow ball connected by black thin lines to the nearest atoms (distances in Å are reported). The zinc bound water molecule necessary for the enzyme catalysed reaction is also represented. (Lower panel) One letter code amino acid sequence of anthrax lethal factor. Amino acids involved in the active site zinc ion coordination are bolded. The residues mutated are shown in a box. Glutamic acids have been mutated to alanine while the tyrosine residue has been mutated to alanine or to phenylalanine. The HExxH zinc-binding motif of zinc endopeptidases is underlined.

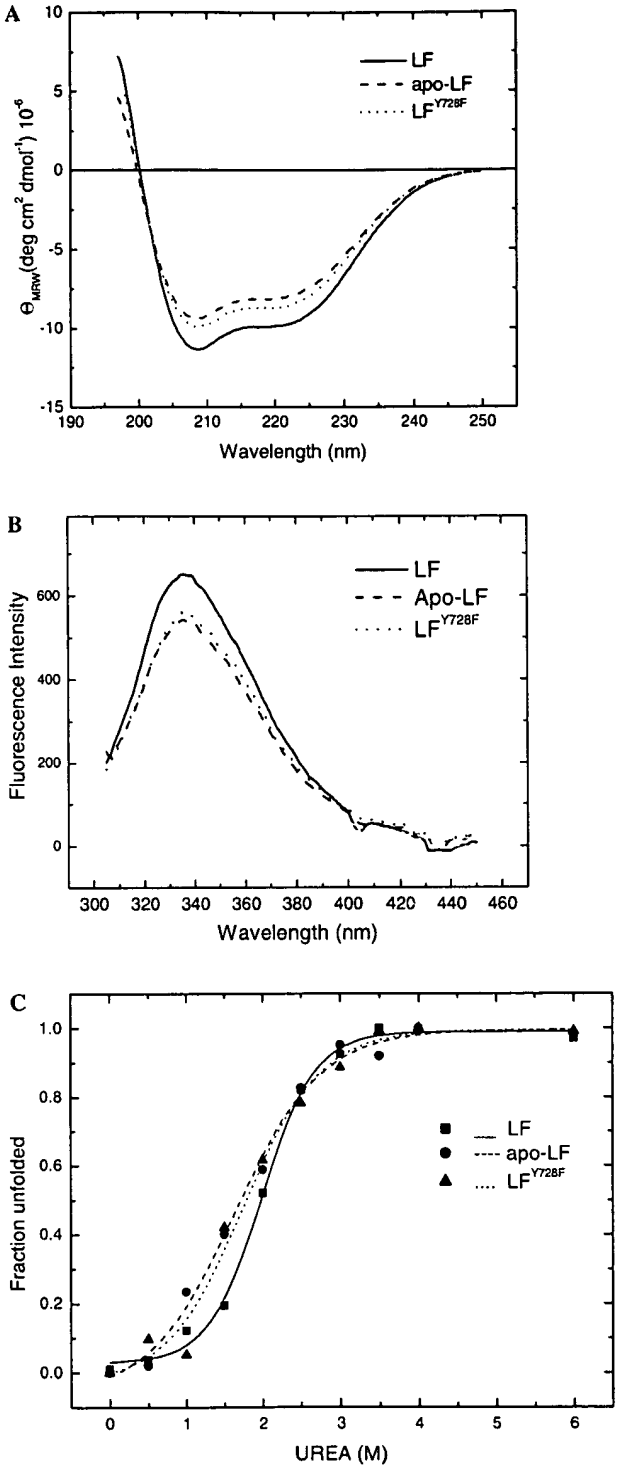

Fig. 2. Spectroscopic analysis of LF and mutants. Far-UV CD, emission fluorescence spectra (λ_{exc} = 280 nm), and denaturation curve of LF, apo-LF, and LF^{Y728F}. The denaturation curves were obtained by monitoring the fluorescence emission at 340 nm, after excitation at 280 nm, in the presence of increasing concentrations of urea. All protein solutions were in Tris–HCl buffer, pH 8.0, 100 mM NaCl. The curves obtained with the other mutants mentioned in the text were all comprised to be between that of apo-LF and that of LF^{Y728F} and are omitted for the sake of clarity.

also produced an alanine-substituted mutant of the fourth zinc ligand Glu-735, LF^{E735A}, and the double mutant $LF^{Y728A;E735A}$. The resulting circular plasmids containing the point mutations were controlled by sequencing and used to transform *E. coli* BL21 cells.

Protein expression and purification

LF and its mutants were expressed in *E. coli* as fusion proteins with GST, affinity purified by GSH–agarose, and the LF chain was released with thrombin. Wild type and mutant proteins were subjected to gel filtration chromatography (Superdex 200, Pharmacia) and analysed by SDS–PAGE under reducing conditions. Results indicate that purification to homogeneity was achieved and that all proteins have identical electrophoretic mobility. This latter result, coupled with the similar expression yields observed for the proteins examined, argues against incorrect protein folding and instability during expression. To prove this point further, a series of spectroscopic analysis was performed on the various proteins including apo-LF (see below).

Zinc content of LF and mutants

The purified recombinant proteins were analysed for their zinc content using atomic absorption spectrometry (Table 1). The native recombinant LF contains about 2 mol of zinc per mole of protein. The zinc content of LF suggests the presence of a second zinc-binding motif [18]. The Y728A and E735A mutants contain only one atom of zinc and the double mutant less than one atom of zinc ion for the protein molecule. This suggests that the mutations destabilize zinc coordination in the active site.

Spectroscopic analysis

To examine whether the mutants are correctly folded, far-UV CD and fluorescence spectroscopy were employed. Near- and far-UV (not shown) CD spectra of the mutants and of apo-LF are similar to that of the wild type LF. The amount of α-helix is in agreement with the one derived from the crystal structure and all

Table 1
Zinc content and melting points of the urea denaturation profiles (see Fig. 2B) of wild type LF, apo-LF, and LF mutants

Protein	Zn^{2+} (mol/mol of protein)	Melting points (urea molarity)
LF	2.0 ± 0.2	2.01 ± 0.05
Apo-LF	0.08 ± 0.01	1.64 ± 0.09
LF^{Y728A}	1.0 ± 0.3	1.71 ± 0.10
LF^{Y728F}	1.5 ± 0.1	1.71 ± 0.05
LF^{E735A}	1.1 ± 0.2	1.82 ± 0.05
$LF^{Y728A;E735A}$	0.8 ± 0.2	1.61 ± 0.05

CD spectra show the characteristic double minimum at 208 and 222 nm, indicating their highly helical nature (Fig. 2A). Near-UV CD spectra of apo-LF, LF, and its mutants present closely similar profiles (not shown). The intensity of the spectrum of recombinant LF is slightly more intense than those of the mutants. The emission fluorescence spectra of LF, apo-LF, and LF mutants obtained after excitation at 280 nm have a maximum of fluorescence intensity at about 332 nm. As in the case of the CD spectra, the intensity of the wild type protein fluorescence is slightly higher than those of the mutants (Fig. 2B). The difference of intensity of the CD and fluorescence spectra indicates that the wild type protein is slightly more rigid than the mutated toxins, suggesting that the active site zinc contributes to the stability of the LF molecule (see also next paragraph).

Urea-induced denaturation curves of apo- and holo-LF and LF mutants

The comparison of urea-induced denaturation curves provides indications on the stability of proteins and on the possible stabilizing effects of bound metal ions or other ligands [25]. Fig. 2C shows the urea denaturation profiles of the holo-LF molecule and of the apo-protein. The fact that a lower urea concentration is needed to unfold the zinc-deprived protein indicates that the metal atom stabilizes the structure of this metalloprotein.

The urea-induced denaturation curves of LF mutants were found to have a melting point slightly lower than that of wild type LF (Fig. 2C and Table 1). This is likely to be due to the fact that Tyr-728 contributes to zinc binding via the interaction of its phenolic ring with the zinc-linked water molecule [16]. The second zinc ion of LF does not appear to stabilize LF because the melting point of apo-LF is not lower than that of the double mutant which contains one atom of zinc per protein molecule.

Proteolytic activity and toxicity of LF and mutants

The zinc-dependent endopeptidase activity of LF can be assayed conveniently in vitro with synthetic peptides mimicking the native substrate and coupled at the C-terminus with either *p*-nitroanilide or with 4-amino-7-methylcoumarin [9]. Fig. 3A shows that the replacement of Tyr-728 and of Glu-735 to alanine completely impairs LF proteolytic activity. Fig. 3B reports an SDS–PAGE of mitogen-activated protein kinase kinase 3 (MKK3) incubated for 2 h at 37 °C in the presence of LF or of its mutants at an enzyme/substrate ratio of 1:20. This analysis shows that LF mutants are enzymatically inactive no matter which substrate is used.

The biological activity of LF mutants was also tested for its capacity of inducing death in cultured macrophages and in Fischer 344 rats in combination with the anthrax protective antigen. Raw macrophage cells treated with PA and LF mutants do not die after 4 h of incubation as do cells treated with wild type recombinant LF. Fischer rats injected intravenously with PA and LF^{Y728F} do not present any symptoms while Fischer rats injected with the same quantities of PA and recombinant LF develop very acute symptoms within 40–50 min.

Discussion

The crystallographic structure of LF [16] provides a firm structural basis for a rational design of mutants addressing the problem of the relation between structure

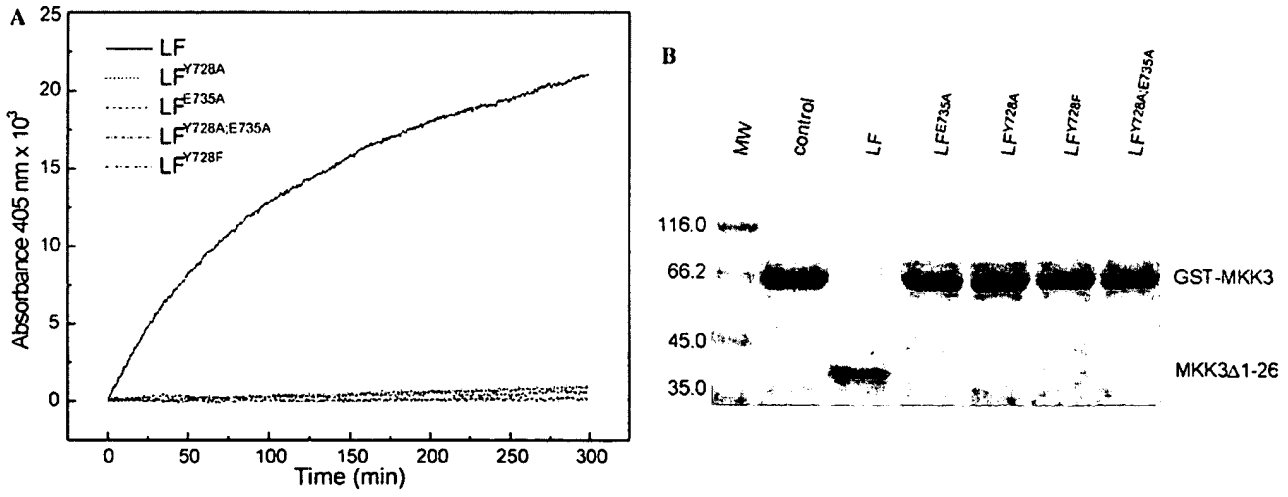

Fig. 3. In vitro proteolytic activity of LF. (A) Kinetics of cleavage of AcYARRRRRRRRVLRpNA by recombinant LF and mutants monitored spectrophotometrically at 405 nm. (B) Proteolysis of recombinant MKK3 in the presence of LF wild type and mutants. The reaction was performed at an enzyme/substrate ratio of 1:20 (w/w) at 37 °C, for 2 h. The reaction products were separated by SDS–PAGE 12% Laemmli.

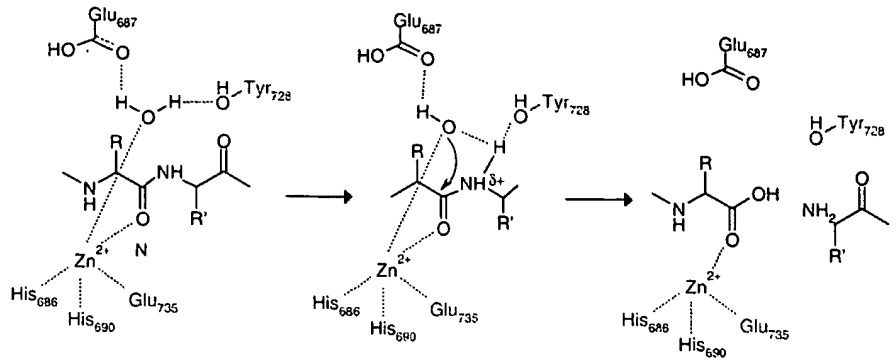

Fig. 4. Proposed mechanism for the anthrax lethal factor-induced proteolysis. The active site is centred around a structural zinc cation coordinated by a strictly conserved HExxH + E motif. Zinc ion is directly coordinated by the two histidines of the motif, by Glu-735 and by a water molecule which forms a strong hydrogen bonding interaction with the Glu of the motif and with the conserved Tyr-728. The phenolic OH group of this residue of LF is absolutely necessary for the hydrolysis reaction as the conservative mutant LF^{Y228F} is completely inactive. We suggest that Tyr-728, in addition to coordinating the catalytic water, stabilizes the amino group of the leaving amino acid, causing a displacement of partial electrostatic charges that weaken the peptide bond, rendering it more susceptible to the nucleophilic attack of the water molecule.

and function in this molecule of paramount importance for human disease and for scientific research.

The present study shows that even the most conservative mutation (LF^{Y728F}) of Tyr-728 leads to a total loss of the activity of the mutated LF which is no longer enzymatically active and does not cause cytolysis of macrophage cells in culture. Strikingly, this mutant is also totally devoid of effect on the Fischer 344 rats which are extremely sensitive to LF [26]. The effect of such mutation is comparable to those of the two Glu residues which directly coordinate the catalytic zinc atom. The crystallographic structure indicates that the OH group of the phenol ring of this tyrosine residue is hydrogen bonded to a water molecule that is bound to zinc. Accordingly, we found that mutation of Tyr-728 led to a diminution of the zinc content. However, such partial loss of zinc cannot per se account for the absolutely complete lack of activity, as determined with very sensitive in vitro and in vivo assays. We are tempted to suggest that this second shell tyrosine residue is also implicated in stabilizing the leaving amino group of the peptide bond undergoing hydrolysis, as depicted in Fig. 4, and that this displacement of charges is very important for the process of peptide bond cleavage.

The comparison of the data of the zinc content of LF and the protein mutants generated here with the urea-induced denaturation curves suggests that the active site zinc atom has a role in stabilizing the structure of this protein, whose native conformation is lost at low urea concentrations. Among the mutants generated here, it is worth mentioning the double Y728A and E735A mutant which is absolutely inactive and cannot revert to produce the wild type LF molecule. This mutant folds similar to LF and could be considered as a candidate component of an anti-anthrax vaccine including detoxified anthrax toxins. This double mutant can be produced in *E. coli* in good amounts in a soluble form.

Acknowledgments

This work was supported by the University of Padova and the Armenise-Harvard Medical School Foundation. We thank Lorenzo Bernardi and Michela Seveso for initial mutagenesis work and Massimo Donà for the help in experiments on Fischer rats.

References

[1] S.H. Leppla, N. Arora, M. Varughese, Anthrax toxin fusion proteins for intracellular delivery of macromolecules, J. Appl. Microbiol. 87 (1999) 284.
[2] D.B. Lacy, R.J. Collier, Structure and function of anthrax toxin, Curr. Top. Microbiol. Immunol. 271 (2002) 61–85.
[3] K.A. Bradley, J. Mogridge, M. Mourez, R.J. Collier, J.A. Young, Identification of the cellular receptor for anthrax toxin, Nature 414 (2001) 225–229.
[4] C.J. Miller, J.L. Elliott, R.J. Collier, Anthrax protective antigen: prepore-to-pore conversion, Biochemistry 38 (1999) 10432–10441.
[5] A. Menard, K. Altendorf, D. Breves, M. Mock, C. Montecucco, The vacuolar ATPase proton pump is required for the cytotoxicity of *Bacillus anthracis* lethal toxin, FEBS Lett. 386 (1996) 161–164.
[6] N.S. Duesbery, C.P. Webb, S.H. Leppla, V.M. Gordon, K.R. Klimpel, T.D. Copeland, N.G. Ahn, M.K. Oskarsson, K. Fukasawa, K.D. Paull, G.F. Vande Woude, Proteolytic inactivation of MAP-kinase-kinase by anthrax lethal factor, Science 280 (1998) 734–737.
[7] G. Vitale, R. Pellizzari, C. Recchi, G. Napolitani, M. Mock, C. Montecucco, Anthrax lethal factor cleaves the N-terminus of MAPKKs and induces tyrosine/threonine phosphorylation of MAPKs in cultured macrophages, Biochem. Biophys. Res. Commun. 248 (1998) 706–711.
[8] G. Vitale, L. Bernardi, G. Napolitani, M. Mock, C. Montecucco, Susceptibility of mitogen-activated protein kinase kinase family members to proteolysis by anthrax lethal factor, Biochem. J. 352 (Pt 3) (2000) 739–745.

[9] F. Tonello, M. Seveso, O. Marin, M. Mock, C. Montecucco, Screening inhibitors of anthrax lethal factor, Nature 418 (2002) 386.
[10] A.M. Friedlander, Macrophages are sensitive to anthrax lethal toxin through an acid-dependent process, J. Biol. Chem. 261 (1986) 7123–7126.
[11] P.C. Hanna, B.A. Kruskal, R.A. Ezekowitz, B.R. Bloom, R.J. Collier, Role of macrophage oxidative burst in the action of anthrax lethal toxin, Mol. Med. 1 (1994) 7–18.
[12] S.O. Kim, Q. Jing, K. Hoebe, B. Beutler, N.S. Duesbery, J. Han, Sensitizing anthrax lethal toxin-resistant macrophages to lethal toxin-induced killing by tumor necrosis factor-alpha, J. Biol. Chem. 278 (2003) 7413–7421.
[13] T.C. Dixon, M. Meselson, J. Guillemin, P.C. Hanna, Anthrax, N. Engl. J. Med. 341 (1999) 815–826.
[14] K.R. Klimpel, N. Arora, S.H. Leppla, Anthrax toxin lethal factor contains a zinc metalloprotease consensus sequence which is required for lethal toxin activity, Mol. Microbiol. 13 (1994) 1093–1100.
[15] A. Menard, E. Papini, M. Mock, C. Montecucco, The cytotoxic activity of *Bacillus anthracis* lethal factor is inhibited by leukotriene A4 hydrolase and metallopeptidase inhibitors, Biochem. J. 320 (Pt 2) (1996) 687–691.
[16] A.D. Pannifer, T.Y. Wong, R. Schwarzenbacher, M. Renatus, C. Petosa, J. Bienkowska, D.B. Lacy, R.J. Collier, S. Park, S.H. Leppla, P. Hanna, R.C. Liddington, Crystal structure of the anthrax lethal factor, Nature 414 (2001) 229–233.
[17] N. Arora, S.H. Leppla, Residues 1–254 of anthrax toxin lethal factor are sufficient to cause cellular uptake of fused polypeptides, J. Biol. Chem. 268 (1993) 3334–3341.
[18] S.K. Kochi, G. Schiavo, M. Mock, C. Montecucco, Zinc content of the *Bacillus anthracis* lethal factor, FEMS Microbiol. Lett. 124 (1994) 343–348.
[19] S.E. Hammond, P.C. Hanna, Lethal factor active-site mutations affect catalytic activity in vitro, Infect. Immun. 66 (1998) 2374–2378.
[20] D.B. Lacy, W. Tepp, A.C. Cohen, B.R. DasGupta, R.C. Stevens, Crystal structure of botulinum neurotoxin type A and implications for toxicity, Nat. Struct. Biol. 5 (1998) 898–902.
[21] L. Li, T. Binz, H. Niemann, B.R. Singh, Probing the mechanistic role of glutamate residue in the zinc-binding motif of type A botulinum neurotoxin light chain, Biochemistry 39 (2000) 2399–2405.
[22] O. Rossetto, P. Caccin, M. Rigoni, F. Tonello, N. Bortoletto, R.C. Stevens, C. Montecucco, Active-site mutagenesis of tetanus neurotoxin implicates TYR-375 and GLU-271 in metalloproteolytic activity, Toxicon 39 (2001) 1151–1159.
[23] M. Rigoni, P. Caccin, E.A. Johnson, C. Montecucco, O. Rossetto, Site-directed mutagenesis identifies active-site residues of the light chain of botulinum neurotoxin type A, Biochem. Biophys. Res. Commun. 288 (2001) 1231–1237.
[24] A. Cataldi, E. Labruyere, M. Mock, Construction and characterization of a protective antigen-deficient *Bacillus anthracis* strain, Mol. Microbiol. 4 (1990) 1111–1117.
[25] C. Nick Pace, A. Bret, S. Thomson, J.A. Thomson, Measuring the conformational stability of a protein, in: T.E. Creighton (Ed.), Protein Structure—A Practical Approach, Oxford University Press, New York, 1993.
[26] J.W. Ezzell, B.E. Ivins, S.H. Leppla, Immunoelectrophoretic analysis, toxicity, and kinetics of in vitro production of the protective antigen and lethal factor components of *Bacillus anthracis* toxin, Infect. Immun. 45 (1984) 761–767.

INFECTION AND IMMUNITY, May 1998, p. 2374–2378
0019-9567/98/$04.00+0

Vol. 66, No. 5

Lethal Factor Active-Site Mutations Affect Catalytic Activity In Vitro

S. E. HAMMOND[1] AND P. C. HANNA[1,2]*

Department of Microbiology[1] and Department of Immunology,[2] Duke University Medical Center, Durham, North Carolina 27710

Received 26 June 1997/Returned for modification 11 August 1997/Accepted 31 January 1998

The lethal factor (LF) protein of *Bacillus anthracis* lethal toxin contains the thermolysin-like active-site and zinc-binding consensus motif HEXXH (K. R. Klimpel, N. Arora, and S. H. Leppla, Mol. Microbiol. 13:1093–1100, 1994). LF is hypothesized to act as a Zn^{2+} metalloprotease in the cytoplasm of macrophages, but no proteolytic activities have been previously shown on any target substrate. Here, synthetic peptides are hydrolyzed by LF in vitro. Mass spectroscopy and peptide sequencing of isolated cleavage products separated by reverse-phase high-pressure liquid chromatography indicate that LF seems to prefer proline-containing substrates. Substitution mutations within the consensus active-site residues completely abolish all in vitro catalytic functions, as does addition of 1,10-phenanthroline, EDTA, and certain amino acid hydroxamates, including the novel zinc metalloprotease inhibitor ZINCOV. In contrast, the protease inhibitors bestatin and lysine CMK, previously shown to block LF activity on macrophages, did not block LF activity in vitro. These data provide the first direct evidence that LF may act as an endopeptidase.

Lethal toxin (LeTx) is a vital virulence factor of *Bacillus anthracis* and has been postulated to act as a Zn^{2+} protease mediating the fatal symptoms observed during anthrax infections by hyperstimulation of host macrophage inflammatory pathways (5, 6, 8, 10). LeTx is an A-B toxin comprised of two distinct proteins. Protective antigen (PA; 735 residues, 82.6 kDa) serves as the B moiety, directing binding to cellular membrane receptors and translocation of its catalytic partners into the cytoplasm (5, 11). Lethal factor (LF; 776 residues, 90.2 kDa) acts as the A moiety (5, 11). Evidence presented by Klimpel et al. demonstrates that LF is a zinc-binding protein which contains the HEXXH motif in its carboxy-terminal (activity) region at residues 686 to 690 ($LF_{686-690}$) (10). They hypothesized that LF requires zinc for activity and perhaps functions as a Zn^{2+}-dependent protease, thus having functions similar to those of, and having an active-site motif in common with, the botulinum and tetanus neurotoxins, albeit with differing cell tropisms, target substrates, and disease sequellae (16). Here, we demonstrate LF-specific, Zn^{2+}-dependent cleavage of synthetic peptides in vitro. These data, as well as those from protease inhibitor profiles, metal ion substitution studies, and mutational analysis of residues within $LF_{686-690}$ that arrest activity, strongly support LF as demonstrating the activities of a Zn^{2+}-dependent neutral endoprotease.

Anthrax toxin purification. LF, PA, and mutants were purified either from *B. anthracis* Sterne or as recombinant proteins from *Escherichia coli* (6–8, 14). *B. anthracis* cultures were grown in defined RM toxin production medium (13). Culture supernatants were sterilized by passage through a 0.22-μm-pore-size filter (Millipore, Bedford, Mass.) and concentrated to 500 ml with the Minitan ultrafiltration system (Millipore). Ammonium sulfate was added to 75%, and the protein pellet was collected and suspended in 20 mM Tris-HCl (pH 8.0) and dialyzed extensively against the same buffer. Very efficient purification was performed by MonoQ anion-exchange fast-performance liquid chromatography (FPLC) (Pharmacia Biotech, Piscataway, N.J.). PA eluted at 130 to 140 mM NaCl, and LF eluted at 250 to 270 mM NaCl. The recombinant proteins expressed in pET15b are produced with an amino-terminal hexa-histidine tag, allowing purification by FPLC affinity chromatography on a HiTrap (Pharmacia Biotech) chelating column. Cultures of *E. coli* BLR(DE3)/pET15b-LF (or indicated LF mutants) were grown in Luria broth containing ampicillin (100 μg ml^{-1}) to an optical density at 600 nm of 0.7 to 1.0, and expression was induced by the addition of IPTG (isopropyl-β-D-thiogalactopyranoside; 1 mM) for 12 h at 18°C. Cell lysates were prepared by French press, cleared by centrifugation, and injected via FPLC (Pharmacia Biotech) onto a HiTrap column charged with Ni^{2+}. Recombinant histidine-tagged LF (wild type [wt] or mutant) eluted at approximately 100 mM imidazole. Eluted protein was further purified by gel filtration on a 320-ml Sephacryl-200 FPLC column. By these methods, PA and LF were each determined to be 95 to 99% pure by sodium dodecyl sulfate-polyacrylamide gel electrophoresis analysis. PA and LF proteins were assayed for cytoxicity activities by a standard ^{51}Cr release assay of a sensitive macrophage cell line (RAW 264.7 ATCC TIB-71) (11, 13). Mutant proteins LF^{E687C}, LF^{H686A}, LF^{H690A}, and $LF^{H686A+H690A}$ were obtained from Kurt Klimpel (10) as direct mutants of wt anthrax LF. LF^{E687D} was created as a recombinant mutant in *E. coli* BLR(DE3) by using the pET15b plasmid and purified as described above.

Protease assay conditions. Oligopeptides were obtained from Sigma. The reaction buffer used was 25 mM potassium phosphate (pH 7.0) containing 20 μM $ZnSO_4$ and 20 μM $CaCl_2$. Each reaction mixture contained as indicated from 250 μM to 1 mM substrate and 0.25 to 2.8 μM enzyme (23 to 250 μg/ml) in a final volume of 100 μl. After incubation at 37°C for 3 to 24 h (as indicated), the reactions were quenched with 1 μl of 10 M HCl and the mixtures were injected onto a C_{18} HP Hypersil-octyldecyl silane column (100 by 4.6 mm, 120-Å pore size, 5-μm particle size) or a C_8 Rainin Microsorb-MV column (250 by 4.6 mm, 300-Å pore size, 5-μm particle size) with a Hewlett-Packard 1050 high-performance liquid chromatography (HPLC) system. The aqueous phase used with the C_{18} column was 25 mM phosphate buffer (pH 7.5) with 2% (vol/

* Corresponding author. Mailing address: Department of Microbiology, Duke University Medical Center, Box 3020, Durham, NC 27710. Phone: (919) 681-6702. Fax: (919) 684-8735. E-mail: hanna@abacus.mc.duke.edu.

vol) methanol (MeOH) and 2% (vol/vol) tetrahydrofuran, and the mobile phase was 100% MeOH. The aqueous phase used with the C_8 column was 0.1% (vol/vol) trifluoroacetic acid (TFA) in water, and the mobile phase was 0.1% (vol/vol) TFA in acetonitrile. Peptide peaks were detected by UV absorption at 215 and 274 nm. For further analysis by mass spectrometry or protein sequencing, peaks were collected as they eluted. For kinetic studies, reaction mixtures of 100 μM to 1 mM substrate with 250 nM LF were run at 25°C. Samples were injected into the HPLC at 3-h intervals. Velocities were then calculated by measuring the reduction of the starting substrate peak over time or by measuring the formation of product peaks over time. In inhibitor studies, enzyme and inhibitors were coincubated at room temperature for 1 h before addition of substrate. For studies with chelating inhibitors, there was no addition of exogenous metals. Otherwise, the conditions were the same as those described above. For pH studies, 250 ng of LF was added to 500 μM substrate in a buffer of 25 mM phosphate with pHs ranging from 5.8 to 8.2. Phosphate buffers were made from appropriate amounts of mono- and dibasic sodium phosphate. Reactions were analyzed after 4 h at 37°C as described above. Results indicated a pH optimum of approximately 6.75, with less than 5% activity at pH 5.5 (results not shown). Thus, the addition of HCl to reaction mixtures was determined to be the best way to quench reactions before HPLC analysis. To create apo-enzyme (no bound metals), purified LF was dialyzed against 10 mM EDTA–1 mM 1,10-phenanthroline for 24 h at 4°C. The proteins were then dialyzed against 20 mM Tris (pH 7.5) in ultrapure water (≥15 MΩ), for 24 h at 4°C, with four buffer changes.

Peptide fragment analysis. Peptides purified by reverse-phase HPLC (RP-HPLC) were analyzed by time-of-flight mass spectrometry. The mass spectrum was recorded by using nitrocellulose targets (9) in an Applied Biosystems Bio-Ion plasma-desorption instrument. The spectrum was accumulated for 10^6 fission events corresponding to approximately 10 min. Further details of the instrumentation and spectral analysis have been described elsewhere (19). Peptide analysis was kindly performed by the Duke Comprehensive Cancer Center Facility, directed by Jan J. Enghild.

Hydrolysis of synthetic peptides. To directly assess whether LF is capable of endopeptidase activity, synthetic peptides (or *p*-nitroanilide-derivatized peptides) as well as a variety of purified proteins were obtained as test substrates in an arbitrary manner. However, the lengths of the synthetic peptides ranged from 2 to 39 residues with efforts to vary both amino acid composition and primary sequence. The overwhelming majority of these substrates were not affected by LF in any discernible way, although they were cleaved by appropriate control proteases (e.g., trypsin, pronase, thermolysin) (data not shown). A complete list of substrates tested in this study is available upon request.

Sixteen oligopeptides 6 to 21 residues in length containing a large variety of amino acids were then obtained and assayed as LF substrates (Table 1). Results presented in Fig. 1 indicate LF cleavage of three peptides. Data illustrated in Fig. 1A show significant hydrolysis of peptide 1 (with ELYENKPRRPYIL hydrolyzed into ELYENKPRRP and YIL) after incubation with LF. The k_{cat}/K_m for this reaction was calculated to be 8.9 s^{-1} M^{-1}. Peptide 2, FGFLPIYRRPAS, was hydrolyzed by LF into the major products FGFLP and IYRRPAS, as well as minor products FGF and LPIYRRPAS (Fig. 1B). The k_{cat}/K_m for this reaction was calculated to be 29.4 s^{-1} M^{-1}. It is important to note that this value reflects the consumption of substrate by both major and minor reactions. Peptide 3, IARRHPYFL, was hydrolyzed by LF into the major products IARRHP and YFL and the minor products IARR and HPYFL (Fig. 1C). Kinetics were not determined for peptide 3; however, the cleavage of peptide 3 occurs faster than that of either peptide 1 or peptide 2 and could have a k_{cat}/K_m value greater than 50 s^{-1} M^{-1}. Unlike peptide 2, in which FGFLP is not split into FGF and LP, the peptide 3 major product IARRHP is hydrolyzed to IARR and HP. These three proteins have some sequence homology at their major cleavage sites, the most notable of which is proline at the new C terminus. The requirement for additional amino acids at key positions is clear from peptides that contain proline but show no signs of cleavage. Additionally, tyrosine is consistently present at or adjacent to the new N-terminal side of the cleavage site. Whether LF requires a tyrosine or simply a bulky uncharged residue is still under investigation. Cleavage of peptide 4 (YGGFLRRI) into YGGFLR and RI is similar to the secondary cleavage of peptide 3, that is, IARRHP to IARR and HP, and occurs at approximately the same rate. Cleavage of peptide 5 (DRVYI HPFHL) occurs extremely slowly into the three products DRV, YIHP, and FHL. No evidence of possible intermediates DRVYIHP and YIHPFDL could be found. Due to the very poor nature of this substrate, drawing similarities between this reaction and the others, while possible, may lead to incorrect assumptions.

The calculated reaction rates are considerably lower than what is normally seen in general metalloproteases such as thermolysin. This may not be unusual considering that tetanus and botulinum neurotoxins, zinc metalloproteases with which LF has active-site homology, are unable to cleave small peptides corresponding to the cleavage sites of their targets. It has been hypothesized that three-dimensional structure plays a more important a role in target specificity than linear amino acid sequence with these neurotoxins (16). It is possible that LF may recognize important structural elements of its target rather than primary sequence, and the relatively slow cleavage of these peptides may demonstrate LF's restriction of its active site to its pertinent cellular target(s). Alternatively, in vivo conditions found within the macrophage may somehow modify

TABLE 1. Peptide substrates used to measure protease activity of anthrax LF

Cleaved peptides[a]	k_{cat}/K_m (s^{-1} M^{-1})[b]
IARR/HP/YFL	50*
FGF/LP/IYRRPAS	29.4
ELYENKPRRP/YIL	8.9
YGGFLR/RI	5*
DRV/YIHP/FHL	0.3*
ELAGAPPEPA	NR
YFLFRPRN	NR
EGLPPRPKIPP	NR
LRRASLG	NR
SYSMEHFRWG	NR
IVPFLGPLLGLLT	NR
GWTLQSAGYLLGPNNFFGLM	NR
ESPLIAKVLTTEPPIITPVRR	NR
HDMNKVLDL	NR
HLGLAR	NR

[a] A slash indicates a known cleavage site as determined by mass spectrometry or peptide sequencing. Peptides were initially chosen at random until the peptide FGFLPIYRRPAS was found to cleave. From then on, peptides were selected for their potential to react with LF.

[b] An asterisk indicates that the k_{cat}/K_m value is estimated. NR, no reaction detected. Kinetics were determined at 25°C with 500 μM substrate and 23 ng of LF/ml (250 nM), and values are averages of two experiments.

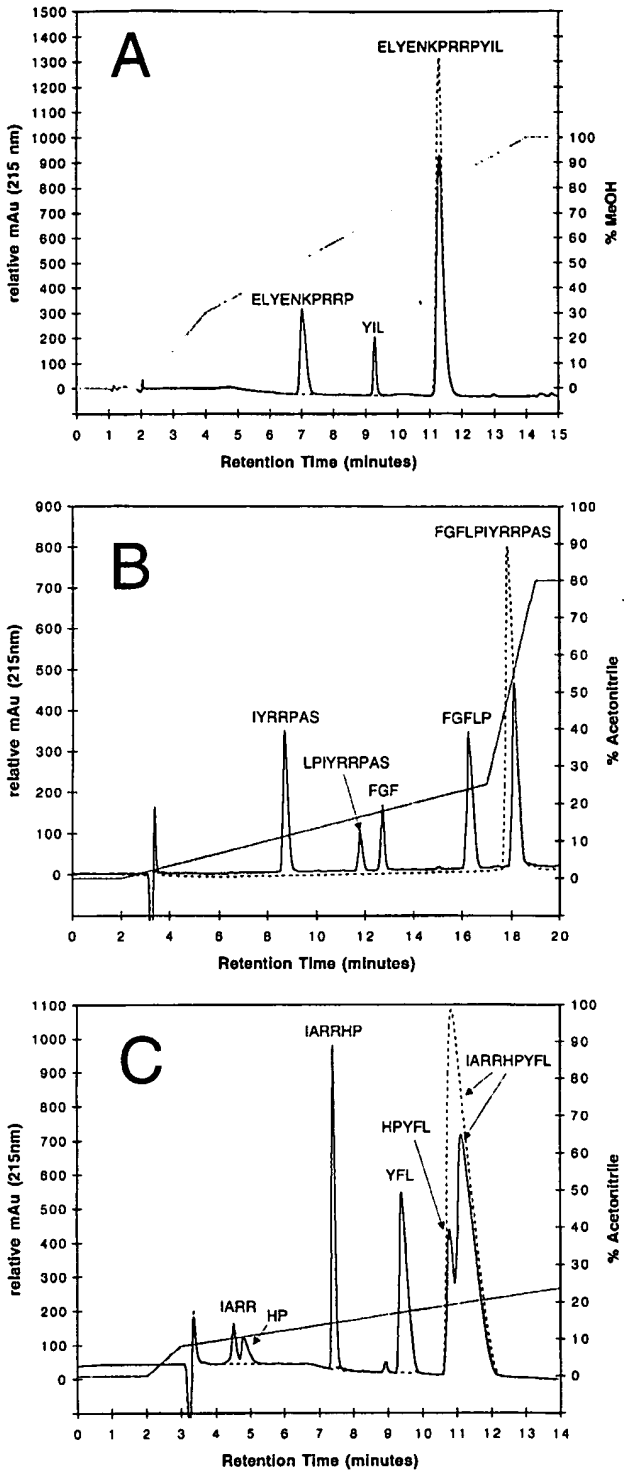

FIG. 1. HPLC elution profiles of synthetic peptides cleaved by anthrax LF. The dashed line represents 500 μM substrate alone without LF, and the solid black line represents substrate plus LF. The gray line indicates percent mobile phase. All reactions occurred at pH 7.0 in 25 mM phosphate buffer. (A) RP-HPLC elution profile of the reaction with peptide 1 (ELYENKPRRPYIL) and 23 ng of LF per ml after 18 h at 37°C. The HPLC running buffer contained 25 mM potassium phosphate (pH 7.5), 2% MeOH, and 2% tetrahydrofuran. (B) Elution profile of the reaction with peptide 2 (FGFLPIYRRPAS) and 250 ng of LF per ml after 4 h at 37°C. The HPLC running buffer was 0.1% TFA in water. The mobile phase was 0.1% TFA in acetonitrile. (C) Elution profile of the reaction with peptide 3 (IARRHPYFL) and 250 ng of LF per ml after 90 min at 37°C. The HPLC running buffer was 0.1% TFA in water. The mobile phase was 0.1% TFA in acetonitrile. All reactions were monitored by UV absorption at 215 nm (see text for more details). The HPLC flow rate was 1.0 ml/min. These results are typical examples of experiments repeated many times.

TABLE 2. Chelator and protease inhibitor profile of anthrax LF

Metal chelator or protease inhibitor	Concn	% Initial activity[a]
Metal chelators		
EDTA	10 mM	0
EDTA	5 mM	6.9
EGTA	5 mM	19.7
1,10-Phenanthroline	1 mM	0
Protease inhibitors		
Alanine hydroxamate	500 μM	>99
Arginine hydroxamate	1 mM	>99
Glutamate γ-hydroxamate	10–500 μM	>99
Glycine hydroxamate	500 μM	>99
Isoleucine hydroxamate	500 μM	>99
Leucine hydroxamate	350 μM	50
Phenylalanine hydroxamate	300 μM	50
Tyrosine hydroxamate	650 μM	50
ZINCOV	350 μM	50
Amastatin	100 μM	>99
Aprotinin	0.05 U	>99
L-Arginine	500 μM	>99
Bestatin	50 μM–1 mM	>99
Calpeptin	75 μM	>99
Captopril	1 mM	>99
Lysine CMK	0.1–1 mM	>99
Nitrobestatin	10 μM	>99
N-Succinyl-L-Proline	100 μM	>99
PMSF[b]	100 μM	>99
Phosphoramidon	500 μM	>99
Tosyl lysine CMK	100 μM	>99
Tosyl phenylalanine CMK	10 μM	>99
Trifluoracetyl LysPro	100 μM	>99
Sodium dodecyl sulfate	1%	0

[a] A 500 μM concentration of peptide 1 (ELYENKPRRPYIL) was mixed with 250 nM of LF mutant and allowed to react for 18 h at 37°C. Samples were then analyzed on an HPLC as described in Materials and Methods. The areas of the substrate and product peaks were measured and compared to that of substrate controls. The results are averages of duplicate experiments.

[b] PMSF, phenylmethylsulfonyl fluoride.

LF to a more active form (e.g., phosphorylation and nicking, etc.).

Inhibitor profiles. LF cleavage of peptides was completely inhibited by the addition of either 1 mM 1,10-phenanthroline or 10 mM EDTA, both of which chelate zinc (Table 2). Activity was partially inhibited by 5 μM EGTA. This indicates that certain metal ions are essential for LF activity in vitro. LF that was cleared of metals through dialysis with EDTA and phenanthroline (see Materials and Methods) showed no propensity to cleave peptides. As individual metals are added back to LF, it is clear that both zinc and calcium are essential for full protease activity (Fig. 2). Additionally, specific amino acid hydroxamates, selective inhibitors of zinc metalloproteases, have been shown to inhibit LF both in vitro and in vivo. Amino acid hydroxamates are reversible inhibitors that fit the enzyme's active site while chelating the zinc ion (3). Tyrosine and leucine hydroxamate showed the best in vitro inhibition with 50% inhibitory concentrations of approximately 300 and 350 μM, respectively. Additionally, ZINCOV, a novel hydrox-

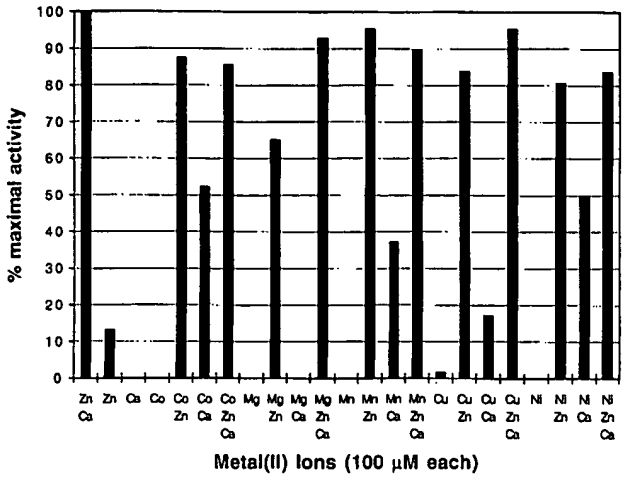

FIG. 2. In vitro protease activity of metal-reconstituted anthrax LF. Comparison of the areas of the major product peaks (see Fig. 1A, peak labeled ELY ENKPRRP) created from the reaction with peptide 1 (ELYENKPRRPYIL) and LF. Reactions of 50 ng of LF per ml with 1 mM ELYENKPRRPYIL occurred at pH 7.0 in 25 mM potassium phosphate buffer containing a 100 μM concentration of the indicated metal(s). Reactions were monitored as described in the text. All metals were chloride salts, except for zinc and nickel which were sulfate salts. After 9 h at 37°C, reaction mixtures were injected into the HPLC. It is important to note that the first three columns indicate the need for both zinc and calcium ions for full catalysis. No reaction was ever observed in the absence of metals, or with calcium alone, cobalt alone, magnesium alone, manganese alone, or nickel alone. The fastest reaction consistently was that in which only zinc and calcium were added. These results are an average of two experiments.

amate, inhibits LF in vitro protease activity at 350 μM and completely protects macrophages in vivo at a concentration of 500 μM (in vivo data not shown). The ability of hydroxamates to inhibit LF supports LF having zinc metalloprotease activity. Further, the specific ability of tyrosine and leucine hydroxamates to inhibit LF may implicate these amino acids as important for active site binding. Previously, relatively high concentrations (200 μM) of the protease inhibitors bestatin and lysine CMK were shown to protect cultured macrophages from lysis by anthrax LeTx (10). In contrast, bestatin and lysine CMK did not inhibit in vitro LF proteolysis of peptides 1 and 2 at concentrations ranging from 50 μM to 1 mM (Table 2), suggesting that the protective effect of these inhibitors observed with LF-challenged cultured cells might not be due to direct inhibition of the toxin's enzymatic activity but rather to some other event in the cytolytic cascade. As an example of this phenomenon, in lipopolysaccharide-stimulated monocytes, inhibitors of metalloproteases were observed to block maturation and release of shock-inducing cytokines (15). It is possible that bestatin and lysine CMK inhibit an event downstream from initial target cleavage by LF. Other classes of protease inhibitors, such as phenylmethylsulfonyl fluoride, *N*-succinyl-L-proline, tosyl lysine CMK, tosyl phenylalanine CMK, and nitrobestatin, did not inhibit LF activity in vitro (Table 2).

Active-site mutations. Amino acid substitutions in $LF_{686-690}$ (the HEXXH motif) were previously shown to be incapable of killing cultured macrophages, suggesting that this region is important for cytotoxicity and perhaps is involved in catalytic function (10). To determine whether this consensus thermolysin-like active-site motif may be directly involved with cleavage of peptides, and to ensure that all hydrolytic activities observed in our assays are specific to LF, amino acid substitutions in $LF_{686-690}$ were tested for the ability to cleave peptides 1 and 2. Mutant toxin molecules assayed were LF^{E687C}, LF^{E687D}, LF^{H686A}, LF^{H690A}, and $LF^{H686A+H690A}$. The recombinant mutants proteins were purified as stable, full-length molecules as determined by sodium dodecyl sulfate-polyacrylamide gel electrophoresis and immunoblot analysis with high-titer polyclonal antitoxin. All histidine mutants were found to have decreased zinc binding as compared to that of wt LF and were unable to kill macrophages in LeTx assays (10; also data not shown). All mutants were mixed individually with peptide 1, 2, or 3 to determine hydrolytic activity. No significant reduction in substrate concentration or generation of cleavage product was observed by RP-HPLC even after 18 h at 37°C (Table 3). This indicates that LF^{H686} and LF^{H690} are important residues for both Zn^{2+} binding and catalysis as well as cytotoxicity. The LF^{E687C} mutant was found to bind zinc at a level equal to that of wt LF yet was also unable to kill cultured cells in LeTx assays (10; also data not shown). However, as with the histidine mutants, LF^{E687C} showed no observable cleavage of peptide 1 even after incubation for 18 h at 37°C (Table 3). Additionally, work with our mutant LF^{E687D} showed no ability to cleave peptides in vitro, even at a very high concentration of enzyme. This mutant was also unable to kill macrophages in vivo (data not shown). This indicates that LF^{E687} is important for cytotoxicity and catalysis but not for Zn^{2+} binding. Importantly, the loss of hydrolytic activities associated with point mutations in the active-site region acts as a control for assignment of hydrolytic functions to LF and not to some undefined contaminating protease.

There were other supporting data for all activities being specific to LF, namely, that LF purified from the supernatant of *B. anthracis* and recombinant LF purified from *E. coli*-soluble extract maintain identical substrate specificities and kinetics (data not shown). For these reasons, it is clear that the observed proteolytic activity is exclusively a property of LF, not of contaminating proteases.

Near the center of the primary amino acid sequence of LF (residues 315 to 416) are five homologous repeats, each 19 amino acids long (Fig. 3). These repeats were first investigated by Quinn et al. (18), who discovered that dipeptide insertions into this region resulted in unstable gene products. Recently, these repeats were proposed to form an EF-hand calcium binding motif (17a; motif reviewed in reference 17) through alignments with sequences of other EF-hand-containing proteins, such as parvalbumin, and an EF-hand consensus sequence (reviewed in reference 17). The results of current metal ion reconstitution experiments are in agreement with this EF-

TABLE 3. Proteolytic activity of anthrax LF mutants

Enzyme	% Cleavage of peptide 1[a]
LF (wt)	85.9
LF (recombinant)	82.1
LF^{H686A}	3.4
LF^{H690A}	3.2
$LF^{H686A+H690A}$	3.0
LF^{E687C}	2.4
LF^{E687D}	0
BSA[b]	0
Trypsin	100
Pronase	100

[a] A 500 μM concentration of peptide 1 (ELYENKPRRPYIL) was mixed with 23 ng (250 nM) of enzyme and allowed to react for 18 h at 37°C. Samples were analyzed on an HPLC as described in Materials and Methods. The areas of the substrate and products peaks were measured and compared to that of substrate controls (no enzyme). The results are averages of duplicate experiments.

[b] BSA, bovine serum albumin.

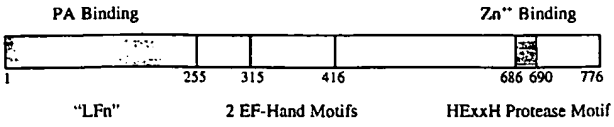

FIG. 3. Known LF domains. The first 255 amino acids are involved in binding to PA, and this region has been termed LFn. This region has a high degree of homology to the first 255 amino acids of anthrax edema factor, which also binds PA. Residues 315 to 416 contain five repeat regions that follow the consensus sequence for two EF-hand calcium-binding motifs (e.g., calmodulin). Residues 686 to 690 contain a thermolysin-like zinc metalloprotease motif HEXXH. Additionally, residues 745 to 749 (HSTDH), which are similar to the inverted zinc metalloprotease motif HXXEH (e.g., insulin-degrading enzyme), could potentially act as another zinc site, either structural or enzymatic.

hand hypothesis and clearly indicate the need for calcium as well as the catalytic zinc to achieve maximum catalysis. EF-hand motifs are the most common calcium binding motifs which are involved mainly in regulation (e.g., calmodulin) and calcium buffering (e.g., parvalbumin) (2). However, only a few EF-hand motifs have been found in prokaryotes, calerythrin being the only well-documented example (1). For this reason, gene transfer has been suggested for the existence of EF-hand motifs in prokaryotes (2). Since LF is likely to contain an EF-hand motif and since gene transfer of bacterial toxins has been a popular hypothesis, especially of ADP-ribosylation toxins (18), it is inviting to suggest that gene transfer is involved with LF. A curious coincidence is that edema factor, an adenylate cyclase that serves as another A domain in anthrax toxin, requires, as a cofactor, calmodulin, an EF-hand-containing protein (12).

B. anthracis LeTx is the major virulence factor responsible for symptoms associated with systemic anthrax (reviewed in references 5 and 11). Although LF, through its association with PA, can bind to and enter the cytoplasm of most cells tested, only macrophages seem to be affected (4). In macrophages, LF induces hyperstimulation of the oxidative burst, expression of proinflammatory cytokines tumor necrosis factor alpha and interleukin 1β, and cytolysis (6, 8). The release of these potent host mediators are responsible for the dramatic hypotension, shock, and death of the victim (6, 8, 11). It is interesting to speculate that the proteolytic activities associated with LF cleave some cytoplasmic protein responsible for regulation of macrophage inflammatory processes. The exact nature of pertinent cellular LF targets and whether proline specificity is maintained within these targets remain to be determined.

We are grateful to Sylvia Hill for providing expert technical assistance and to Carlo Petosa, Terry Dixon, and John Ireland for useful discussions.

This study was supported in part by National Institutes of Health grants AI08649 and AI40644, American Cancer Society grant ACS-IRG158K, and funds from the Duke University Medical Center.

Editor: J. T. Barbieri

REFERENCES

1. **Bylsma, N., T. Drakenberg, I. Anderson, P. F. Leadlay, and S. Forsen.** 1992. Prokaryotic calcium-binding protein of the calmodulin superfamily. Calcium binding to a *Saccharopolyspora erythraea* 20kDa protein. FEBS Lett. **299**:44–47.
2. **Celio, M. R.** 1996. Guidebook to the calcium-binding proteins. Oxford University Press, New York, N.Y.
3. **Chan, W. W. C., P. Dennis, W. Demmer, and K. Brand.** 1982. Inhibition of leucine aminopeptidase by amino acid hydroxamates. J. Biol. Chem. **257**: 7955–7957.
4. **Friedlander, A. M.** 1986. Macrophages are sensitive to anthrax lethal toxin through an acid-dependent process. J. Biol. Chem. **261**:7123–7126.
5. **Hanna, P. C.** 1998. Anthrax pathogenesis and host response. Curr. Top. Microbiol. Immunol. **225**:13–35.
6. **Hanna, P. C., D. Acosta, and R. J. Collier.** 1993. On the role of macrophages in anthrax. Proc. Natl. Acad. Sci. USA **90**:10198–10201.
7. **Hanna, P. C., S. Kochi, and R. J. Collier.** 1992. Biochemical and physiological changes induced by anthrax lethal toxin in J774 macrophage-like cells. Mol. Biol. Cell **3**:1269–1277.
8. **Hanna, P. C., B. A. Kruskal, R. Allen, B. Ezekowitz, B. R. Bloom, and R. J. Collier.** 1994. Role of macrophage oxidative burst in the action of anthrax lethal toxin. Mol. Med. **1**:7–18.
9. **Jonsson, G. P., A. B. Hodin, P. L. Häkansson, B. V. R. Sundqvist, B. G. S. Säve, P. F. Nielson, P. Roepstorff, K. E. Johansson, I. Kamensky, and M. S. L. Lindborg.** 1986. Plasma desorption mass spectrometry of peptides and proteins adsorbed on nitrocellulose. Anal. Chem. **58**:1084.
10. **Klimpel, K. R., N. Arora, and S. H. Leppla.** 1994. Anthrax toxin lethal factor contains a zinc metalloprotease consensus sequence which is required for lethal toxin activity. Mol. Microbiol. **13**:1093–1100.
11. **Leppla, S. H.** 1995. Anthrax toxins: bacterial toxins and virulence factors in disease. Marcel Dekker, Inc., New York, N.Y.
12. **Leppla, S. H.** 1984. *Bacillus anthracis* calmodulin-dependent adenylate cyclase: chemical and enzymatic properties and interactions with eukaryotic cells. Adv. Cyclic Nucleotide Protein Phosphorylation Res. **17**:189–198.
13. **Leppla, S. H.** 1988. Production and purification of anthrax toxin. Methods Enzymol. **165**:103–116.
14. **Milne, J. C., S. R. Blanke, P. C. Hanna, and R. J. Collier.** 1995. Protective antigen-binding domain of anthrax lethal factor mediates translocation of a heterologous protein fused to its amino- or carboxy-terminus. Mol. Microbiol. **15**:661–666.
15. **Mohler, K. M., P. R. Sleath, J. N. Fitzner, D. P. Cerretti, M. Alderson, S. S. Kerwar, D. S. Torrance, C. Otten-Evans, T. Greenstreet, K. Weerawarna, S. R. Kronheim, M. Petersen, M. Gerhart, C. J. Kozlosky, C. J. March, and R. A. Black.** 1994. Protection against a lethal dose of endotoxin by an inhibitor of tumour necrosis factor processing. Nature **370**:218–220.
16. **Montecucco, C., and G. Schiavo.** 1994. Mechanism of action of tetanus and botulinum neurotoxins. Mol. Microbiol. **13**:1–8.
17. **Nakayama, S., and R. H. Kretsinger.** 1994. Evolution of EF-hand proteins. Annu. Rev. Biophys. Biomol. Struct. **23**:473–507.

17a. **Petosa, C.** Personal communication.

18. **Quinn, C. P., Y. Singh, K. R. Klimpel, and S. H. Leppla.** 1991. Functional mapping of anthrax toxin lethal factor by in-frame insertion mutagenesis. J. Biol. Chem. **266**:20124–20130.
19. **Sundqvist, B., I. Kamensky, P. Hakansson, J. Kjellberg, M. Salehpour, S. Widdiyasekera, J. Fohlman, P. A. Peterson, and P. Roepstorff.** 1984. Californium-252 plasma desorption time of flight mass spectroscopy of proteins. Biomed. Mass. Spectrom. **11**:242–257.

JOURNAL OF BACTERIOLOGY, Apr. 1999, p. 2358–2362
0021-9193/99/$04.00+0

Vol. 181, No. 8

Genetic Diversity in the Protective Antigen Gene of *Bacillus anthracis*

LANCE B. PRICE,[1] MARTIN HUGH-JONES,[2] PAUL J. JACKSON,[3] AND PAUL KEIM[1]*

Department of Biological Science, Northern Arizona University, Flagstaff, Arizona 86011-5640[1]; Department of Epidemiology and Community Health, School of Veterinary Medicine, Louisiana State University, Baton Rouge, Louisiana 70803[2]; and Environmental Molecular Biology Group, Los Alamos National Laboratory, Los Alamos, New Mexico 87545[3]

Received 2 December 1998/Accepted 29 January 1999

***Bacillus anthracis* is a gram-positive spore-forming bacterium that causes the disease anthrax. The anthrax toxin contains three components, including the protective antigen (PA), which binds to eucaryotic cell surface receptors and mediates the transport of toxins into the cell. In this study, the entire 2,294-nucleotide protective antigen gene (*pag*) was sequenced from 26 of the most diverse *B. anthracis* strains to identify potential variation in the toxin and to further our understanding of *B. anthracis* evolution. Five point mutations, three synonymous and two missense, were identified. These differences correspond to six different haploid types, which translate into three different amino acid sequences. The two amino acid changes were shown to be located in an area near a highly antigenic region critical to lethal factor binding. Nested primers were used to amplify and sequence this same region of *pag* from necropsy samples taken from victims of the 1979 Sverdlovsk incident. This investigation uncovered five different alleles among the strains present in the tissues, including two not seen in the 26-sample survey. One of these two alleles included a novel missense mutation, again located just adjacent to the highly antigenic region. Phylogenetic (cladistic) analysis of the *pag* corresponded with previous strain grouping based on chromosomal variation, suggesting that plasmid evolution in *B. anthracis* has occurred with little or no horizontal transfer between the different strains.**

Bacillus anthracis is the causative organism of the potentially fatal disease anthrax. Virulent forms of *B. anthracis* carry two large plasmids, pX01 (ca. 174 kb) and pX02 (ca. 95 kb). Virulence factors include toxin and capsule production, encoded on pX01 and pX02, respectively. The anthrax toxin is composed of three proteinaceous subunits: (i) lethal factor (LF), the toxin component thought to kill host cells by disrupting the mitogen-activated protein kinase pathway (2); (ii) edema factor (EF), an adenylyl cyclase that causes skin edema in the infected host (6); and (iii) protective antigen (PA), which binds to eucaryotic cell surface proteins, forms homoheptamers, and then binds to and internalizes EF and LF.

The structure and function of PA have been well described. The entire PA gene (*pag*) sequence has been published and is available in GenBank (accession no. M22589) (12). The three-dimensional structure has also been solved and is available in the NCBI Entrez 3D database (MMDB no. 6980) (10). Finally, antibody-binding experiments have been used to define regions of the PA protein critical to cell surface attachment as well as LF binding (8). Missing from the literature until now was a population study of *pag* from diverse strains of *B. anthracis* to define the natural variation in this important gene.

In past studies, plasmid-specific genetic variation in *B. anthracis* has been largely ignored. A recent population study, based on chromosomal markers, demonstrated that *B. anthracis* is one of the most monomorphic bacterial species known (5). This chromosomal amplified fragment length polymorphism study examined ca. 6.3% of the *B. anthracis* genome for length variations and ca. 0.36% for point mutations. However, due to ambiguities arising from the absence of one or both of the plasmids, plasmidal data were omitted from the final results. Studies of pX01 diversity and especially of *pag* are essential to understanding evolution of pathogenesis in *B. anthracis*. Likewise, comparative studies of plasmid-based versus chromosomal variation can provide insight into the frequency of horizontal plasmid transfer in natural *B. anthracis* populations.

In this study we have sequenced the entire *pag* gene from 26 of the most diverse strains of *B. anthracis* (5). These sequences were aligned and analyzed for point mutations then studied phylogenetically to determine if the *pag* data are consistent with chromosomal diversity groups. Additionally, we sequenced a 307-bp variable region of *pag* from 10 Sverdlovsk anthrax victim necropsy samples (4) in order to identify novel *pag* sequences.

MATERIALS AND METHODS

***B. anthracis* DNA.** Culture conditions, DNA isolation methods, and diversity groups are described in reference 5. Necropsy tissue DNA was isolated as described by Jackson et al. (4).

PCR amplification of DNA. Table 1 contains the sequences for all primers used for this project. These were designed from the published *pag* sequence (GenBank accession no. M22589) and synthesized by Gibco/BRL, Bethesda, Md. All primer positions cited throughout this report are based on this GenBank sequence. Two DNA fragments, together totaling 2,531 bp of sequence, were initially amplified to provide a *pag* sequencing template from the 26 *B. anthracis* strains. PA-1F and PA-1R were used to amplify a 1,191-bp fragment containing the 5′ portion of PA. This included 131 bp of upstream flanking sequence. PA-2F and PA-2R were used to amplify a 1,449-bp fragment containing the 3′ portion of PA. This included 106 bp of downstream flanking sequence. The two fragments contained 109 bp of overlapping sequence near the middle of the gene. Fifty-microliter PCR mixtures contained 1× PCR buffer (20 mM Tris [pH 8.4], 50 mM KCl; Gibco/BRL), 0.10 mM deoxynucleoside triphosphates, 4 mM $MgCl_2$, ~0.2 ng of template DNA per μl, 0.04 U of *Taq* DNA polymerase (Gibco/BRL) per μl, and 0.4 μM forward and reverse primers, adjusted to 50 μl with filtered (0.2-μm-pore-size filter) 17.8 mohm E-pure water. Reactions were heated to 94°C for 5 min and then subjected to 35 cycles, each consisting of 30 s at 94°C, 30 s at 62°C, and 1.5 min at 72°C. This was followed by heating to 72°C for 5 min to complete primer extension. PCR products were purified through

* Corresponding author. Mailing address: Department of Biological Sciences, Northern Arizona University, Flagstaff, AZ 86011-5640. Phone: (520) 523-1078. Fax: (520) 523-7500. E-mail: Paul.Keim@nau.edu.

TABLE 1. Primers used in this study

Primer	Type[a]	Sequence (5'→3')	Position[b]	Amplicon size (bp)
PA-1F	Amp/Seq	ATA TTT ATA AAA GTT CTG TTT AAA AAG CC	5'-1673	1,191
PA-1R	Amp/Seq	TAA ATC CTG CAG ATA CAC TCC CAC	3'-2840	1,191
PA-2F	Amp/Seq	ATA AGT AAA AAT ACT TCT ACA AGT AGG ACA C	5'-2755	1,449
PA-2R	Amp/Seq	GAT TTA GAT TAC TGT TTA AAA CAT ACT CTC C	3'-4173	1,449
PA-3	Seq	TCA TGT AAC AAT GTG GGT AGA TGA C	5'-2145	NA[c]
PA-4	Seq	CTC TAT GAG CCT CCT TAA CTA CTG AC	3'-3717	NA
PA-5F	Amp	ATC CTA GTG ATC CAT TAG AAA CGA C	5'-3416	330
PA-5R	Amp	CTT CTC TAT GAG CCT CCT TAA CTA CTG	3'-3719	330
PA-5F$_{nest}$	Amp/Seq	AGT GAT CCA TTA GAA ACG AC	5'-3421	307
PA-5R$_{nest}$	Amp/Seq	TAA CTA CTG ACT CAT CCG C	3'-3709	307

[a] Amp, used for amplification; Seq, used for sequencing; Amp/Seq, used for both amplification and sequencing.
[b] All correspond to GenBank accession no. M22589 nucleotide positions.
[c] NA, not applicable.

Qiaquick purification minicolumns (Qiagen Inc., Valencia, Calif.) and then quantified on ethidium bromide-stained 1.25% agarose-Tris-acetate-EDTA gels. These purified fragments were then used in subsequent sequencing reactions. PCR amplification of necropsy sample DNA was performed as described by Jackson et al. (4), using primers PA-5F, PA-5R, PA-5F$_{nest}$, and PA-5R$_{nest}$ (Table 1).

DNA sequencing. PCR products were sequenced on an ABI model 377 fluorescence sequencer using a PRISM Ready Reaction BigDye terminator cycle sequencing kit (both from Perkin-Elmer/Applied Biosystems Inc., Foster City, Calif.). Sequences were aligned and analyzed with Sequence Navigator software (Perkin-Elmer/Applied Biosystems).

Cladistic analysis. Cladistic analysis was performed on the *pag* sequences by using maximum parsimony with PAUP 3.1.1 software (developed by David L. Swofford, Illinois Natural History Survey) and manual examinations of sequence polymorphisms.

Three-dimensional analysis. The PA structure has been solved and is available on the NCBI Entrez 3D database (MMDB no. 6980) (10). Amino acid residues shown to vary among strains were identified on the three-dimensional structure, and then physical distances from the putative LF binding region of PA domains 3 and 4 were estimated by using MAGE 4.5 software (developed by David Richardson, Biochemistry Department, Duke University, Durham, N.C.).

RESULTS

Sequence alignment of the entire PA gene from 26 strains representative of the five *B. anthracis* diversity groups (5) (Table 2) revealed five point mutations, three synonymous and two missense, shown in Table 3. All five mutations are transitions. Two of the synonymous mutations occur only once. However, the other differences are present with frequencies ranging from 3/26 to 20/26. The two missense mutations are located adjacent to a highly antigenic region crossing the junction between PA domains 3 and 4 shown to be critical to LF binding (Fig. 1) (8, 10). The different mutational combinations observed in this

TABLE 2. *B. anthracis* strains used in this study

Strain	Geographic origin or description	Diversity group[a]	PA genotype[b]	PA phenotype[c]
BA0052	Jamaica	Sterne-Ames	I	FPA
BA1087	Scotland	Sterne-Ames	I	FPA
J611	Indonesia	Sterne-Ames	I	FPA
BA1031	South Africa	Sterne-Ames	I	FPA
BA1043	South Africa	Sterne-Ames	I	FPA
28	Ohio	Sterne-Ames	II	FPA
MOZ-3	Mozambique	Southern Africa	III	FPA
BA1035	South Africa	Southern Africa	III	FPA
33	South Africa	Southern Africa	IV	FPA
A24	Slovakia	Southern Africa	V	FPV
K20	South Africa (Kruger)	Kruger	V	FPV
26/05/94	Zambia	Kruger	V	FPV
BA1033	South Africa	WNA	V	FPV
BA1017	Haiti	WNA	V	FPV
BA1015	Maryland	WNA	V	FPV
93-194C	Canada	WNA	V	FPV
93-195C-8	Canada	WNA	V	FPV
BA1040	Colorado	WNA	V	FPV
BA1007	Iowa	WNA	V	FPV
2/6	Turkey	WNA	V	FPV
Pak-2	Pakistan	WNA	V	FPV
STI-1	Russian vaccine strain	WNA	V	FPV
F-1	South Korea	Vollum	V	FPV
BA1024	Ireland	Vollum	VI	FSV
ASC-3	United Kingdom	Vollum	VI	FSV
BA1009	Pakistan	Vollum	VI	FSV

[a] Diversity designations are consistent with those described by Keim et al. (5).
[b] Described in Table 4.
[c] Designated by the single-letter designations of the three amino acids shown to vary in this study.

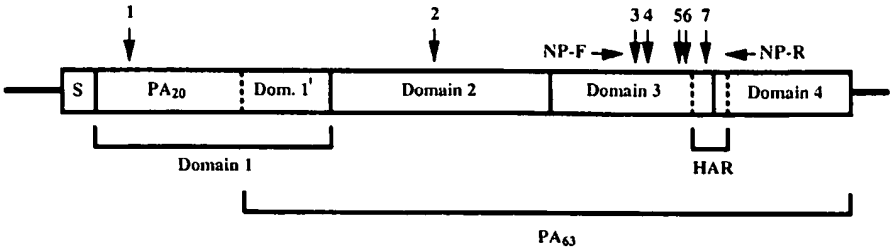

FIG. 1. Model of *pag* from *B. anthracis*. S, region of gene that codes for cleaved signal region; NP-F and NP-R, forward and reverse nested primers used to amplify variable regions from the Sverdlovsk tissue samples; black vertical arrows, missense mutations; grey vertical arrows, synonymous mutations; HAR, highly antigenic region important to LF binding (8, 10). Dom., domain.

study give rise to six PA genotypes and three PA phenotypes (Table 4).

Cladistic analysis of the 26 *pag* sequences was performed by the maximum parsimony method to produce a gene tree (Fig. 2A). The 26 strains grouped into four clades of 3, 3, 6, and 14 individuals. These groups were defined by three synapomorphic (informative) differences. In addition, we identified two apomorphic (uninformative) nucleotide differences (mutations 2 and 6) that separated two strains (28 and 33) from others in their clades. These mutations are identified on the respective branches but were not used to isolate these strains from their groups. The clades and topology identified by this tree were mostly congruent with those generated from chromosomal markers (Fig. 2B) (5). The only aberrations are the following. (i) Chromosomal data from strain A24 indicate that it is of the Southern Africa lineage (5), but the *pag* data place this strain with the Western North America (WNA) diversity group (one mutational step away); (ii) chromosomal data from strain F-1 indicate that it is of the Vollum lineage, but the *pag* data place this strain with the WNA diversity group (again, one mutational step away); and (iii) chromosomal markers indicate that the Kruger samples, although very similar, are genetically distinct from the WNA lineage. However, the *pag* gene tree did not resolve these two distinct groups. It should be noted that chromosomal markers indicate that Vollum and WNA are sister groups and, likewise, that Kruger and WNA are closely related. Only with strain A24 do the *pag* data suggest that strains from two distantly related groups (based on chromosomal markers) are closely related.

To determine the *pag* genotypes and phenotypes of the strain(s) involved in the Sverdlovsk incident, nested PCR primers (Table 1) were designed to amplify and sequence a 307-bp region of *pag*. This region spans the junction between PA domains 3 and 4 where much of the variation was observed. This analysis uncovered two additional transition mutations (3 and 7 in Table 3). One was synonymous, while the other was a novel missense mutation resulting in a phenylalanine↔leucine change. These changes resulted in two additional genotypes and one new phenotype (Table 4). The amino acid change was, again, immediately adjacent to the highly antigenic region of PA domains 3 and 4 (Fig. 1). Repetitive sequencing of these tissues uncovered multiple PA genotypes within some of the individual necropsy samples. Together, five different PA genotypes were observed in the Sverdlovsk samples, with some samples showing evidence of infection by multiple strains (Table 5). This finding is consistent with the results of Jackson et al. (4).

Figure 3 is an unrooted phylogenetic tree demonstrating the five mutational steps leading to the six PA genotypes and three PA phenotypes identified in this study. Additionally, the putative positions of the Sverdlovsk samples are shown. However, because the Sverdlovsk identifications were based on just the 307-bp region around the antigenic portion of PA domains 3 and 4, these placements are only tentative.

Three-dimensional analysis of all the amino acid changes observed in this study (mutations 3, 4, and 5 in Table 3) indicated that these changes are not only close sequentially but also very close in three-dimensional space to the antigenic region important for LF binding. Mutation 3 (Phe to Leu), is ca. 11.2 Å, mutation 4 (Pro to Ser) is ca. 20.3 Å, and mutation 5 (Ala to Val) is ca. 19.0 Å from the central portion of this

TABLE 3. Mutations identified in this study

Mutation	Nucleotide position[a]	Base change	Frequency	Amino acid change
1	1998	C⇔T	20/26	Synonymous
2	2883	G⇔A	1/26	Synonymous
3	3481	T⇔C	NA[b]	F⇔L
4	3496	C⇔T	3/26	P⇔S
5	3602	C⇔T	17/26	A⇔V
6	3606	T⇔C	1/26	Synonymous
7	3672	A⇔G	NA	Synonymous

[a] Nucleotide positions are based on the 4,235-bp pX01 sequence from Sterne strain, accession no. M22589, containing *pag* in its entirety.
[b] NA, not applicable (mutation was observed only in the Sverdlovsk samples).

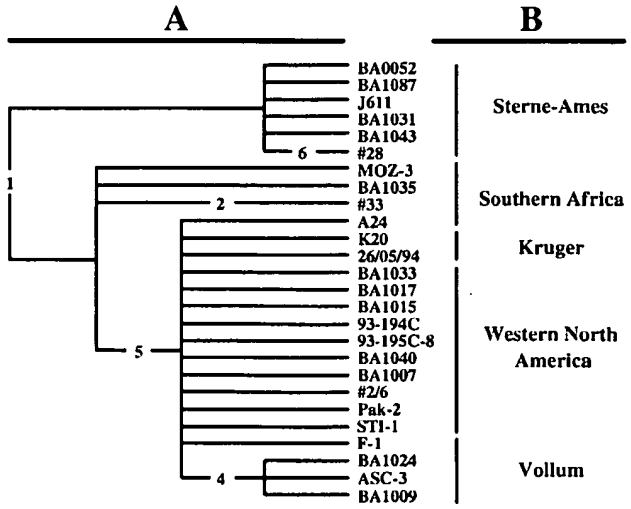

FIG. 2. Cladistic analysis of the 26 diverse strains. (A) Unrooted, maximum parsimony gene tree based on *pag* data developed in this study; (B) strain diversity groups based on chromosomal AFLP data described by Keim et al. (5). Branch mutations are numbered as described for Table 3.

TABLE 4. PA genotypes and phenotypes identified in this study[a]

PA genotype	PA phenotype[b]	Genotypic frequency	Mutation[c]						
			1	2	3	4	5	6	7
I	FPA	5/26	C	G	T(F)	C(P)	C(A)	T	A
II	FPA	1/26	C	G	T(F)	C(P)	C(A)	C	A
III	FPA	2/26	T	G	T(F)	C(P)	C(A)	T	A
IV	FPA	1/26	T	A	T(F)	C(P)	C(A)	T	A
V	FPV	14/26	T	G	T(F)	C(P)	T(V)	T	A
VI	FSV	3/26	T	G	T(F)	T(S)	T(V)	T	A
VII_{Svd}	LPA	NA	—	—	C(L)	C(P)	C(A)	T	A
$VIII_{Svd}$	FPA	NA	—	—	T(F)	C(P)	C(A)	T	G

[a] NA, not applicable (mutation was seen only in the Sverdlovsk samples); —, the region was not analyzed for the Sverdlovsk sample.
[b] Designated by the single-letter designation of the three amino acids shown to vary.
[c] Described in Table 3.

region. These spatial distances were estimated solely on peptide backbone-to-peptide backbone relationships. However, when the three-dimensional spaces occupied by the side chains of the amino acids were considered, changes were found to affect residues as close as 6.9 Å from the central amino acids of this critical antigenic region.

DISCUSSION

The protective antigen protein is central to the virulence associated with anthrax toxin. Elucidation of PA variation and its encoding gene could lead to a better understanding of *B. anthracis* virulence and evolution. Until now, *pag* had been sequenced in its entirety only from a single *B. anthracis* strain (12). In this study, a detailed analysis of the entire *pag* sequence (2,294 bp) from 26 diverse *B. anthracis* strains revealed only five point mutations, corroborating the high degree of genetic monomorphism found by Keim et al. (5).

Among these mutations, there is a disproportionate number of missense (two) to synonymous (three) changes. A common ratio of missense to synonymous mutations is approximately 1:5; here we see a ratio more than threefold greater (7). These missense mutations are located near a highly antigenic region, critical to LF binding. In monoclonal antibody studies, Little et al. demonstrated that by blocking an epitope between amino acids Ile-581 and Asn-601 (Fig. 1), they could effectively block LF binding to PA (8). Three-dimensional analysis indicated that the missense mutations identified in our study are very close in three-dimensional space to this antigenic region. While none of the three missense mutations were dramatic, such as a change from an extremely hydrophobic to a hydrophilic amino acid, the proline-to-serine change has the potential to make important three-dimensional alterations, since proline isomerization is known to play a critical role in protein folding. Because of their close proximity, these amino acid changes have the potential to effect LF binding, either directly or indirectly, within an infected host. The grouping of these missense mutations near this antigenic region and the disproportionate number of missense to synonymous mutations suggests adaptive variation. One of the two new mutations identified in the Sverdlovsk victims' tissues was found to be a novel missense mutation located, sequentially and three dimensionally, near the highly antigenic region of the junction between PA domains 3 and 4. When these mutations are included with those identified in the 26-sample survey, the ratio of missense to synonymous mutation is increased to 3.8:5.

The amplification and sequencing of the 307-bp *pag* fragment from the Sverdlovsk tissue samples suggested that at least five different strains of *B. anthracis* were present in the samples and that some of the individual victims had been infected with multiple strains. These data corroborate earlier work with the *vrrA* locus that suggested that multiple strains of anthrax had been released during the 1979 incident (1, 4). Besides the Russian vaccine strain STI-1, included in this study, these tissue samples are a rare glimpse at the different strains of *B. anthracis* that are thought to be endemic in the vast region of the former Soviet Union. The fact that two previously unobserved mutations were found in the Sverdlovsk samples stresses the importance of collecting and analyzing *B. anthracis*

TABLE 5. Tissue samples from Sverdlovsk victims analyzed in this study[a]

Sample	Tissue	PA genotype(s)	PA phenotype(s)
7.RA93.15.15	Spleen	V	FPV
40.RA93.40.5	Spleen	VI, VII_{Svd}	FSV, LPA
27.RA93.30.3	Spleen	V	FPV
37.RA93.35.4	Vaccination site	I,[b] V	FPA, FPV
37.RA93.35.6	Lung	$VIII_{Svd}$	FPA
3.RA93.1.1	Meninges	$VIII_{Svd}$	FPA
25.RA93.031	Meninges	V	FPV
1.RA93.42.1	Meninges	V	FPV
33.RA93.20.5	Meninges	V	FPV
21.RA93.38.4	Lymph node	V	FPV

[a] Determination of PA genotypes and phenotypes was based solely on the 307-bp region connecting PA domains 3 and 4. Multiple strains were identified in some tissues.
[b] Due to the limited region analyzed, this strain may be type I, II, or IV but was grouped with I for simplicity.

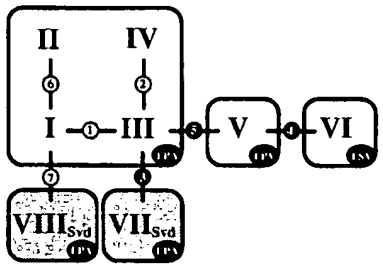

FIG. 3. Unrooted phylogenetic tree of PA genotypes. Open boxes show the three PA phenotypes identified; shaded boxes show the possible positions of the Sverdlovsk genotypes, VII_{Svd} and $VIII_{Svd}$. Synonymous mutations are shown in open circles, and missense mutations are shown in closed circles. Each mutation is described in Table 3 and the phenotypes are described in Table 4.

strains from areas where anthrax is endemic but largely uncharacterized by molecular genetic analysis.

Independent cladistic analysis of pX01 by using the *pag* sequence has enabled us to estimate the likelihood of horizontal transfer of this plasmid between different *B. anthracis* strains in natural populations. Although horizontal transfer in *Bacillus* spp. is possible under laboratory conditions, the similarity of the cladistic grouping from the *pag* data to that of the chromosomal markers suggests that the differences in *pag* arose from evolution within particular strain lineages and were not a result of horizontal pX01 transfer. The single possible exception is associated with the A24 sample, which chromosomally is related to the Southern Africa strains, while the *pag* data for this strain are consistent with Kruger-WNA. This is either a result of convergent evolution or evidence of horizontal pX01 transfer. Further, it should be noted that the data presented in this report do not rule out the potential for horizontal transfer of plasmid pX01 between closely related strains within an infected host.

The unrooted phylogenetic tree (Fig. 3) is a useful tool for demonstrating the relationships between the different PA genotypes. However, it is not meant to infer an evolution toward a particular form of PA. Although distant homologues from other gram-positive bacteria are cited (3, 9, 11), none of these is close enough to root a *B. anthracis* PA phylogenetic tree. Without an ancestral PA sequence, one is unable to determine which PA phenotypes are ancestral and which are derived.

ACKNOWLEDGMENTS

We thank James M. Schupp, Kimothy L. Smith, Debra M. Adair, and Karen K. Hill for technical support.

REFERENCES

1. **Andersen, G. L., J. M. Simchock, and K. H. Wilson.** 1996. Identification of a region of genetic variability among *Bacillus anthracis* strains and related species. J. Bacteriol. **178**:377–384.
2. **Duesbery, N. S., C. P. Webb, S. H. Leppla, V. M. Gordon, K. R. Klimpel, T. D. Copeland, N. G. Ahn, M. K. Oskarsson, K. Fukasawa, K. D. Paull, and G. F. Vande Woude.** 1998. Proteolytic inactivation of MAP-kinase-kinase by anthrax lethal factor. Science **280**:734–737.
3. **Gibert, M., S. Perelle, G. Daube, and M. R. Popoff.** 1997. *Clostridium spiroforme* toxin genes are related to *C. perfringens* iota toxin genes but have a different genomic localization. Syst. Appl. Microbiol. **20**:337–347.
4. **Jackson, P. J., M. E. Hugh-Jones, D. M. Adair, G. Green, K. K. Hill, C. R. Kuske, L. M. Grinberg, F. A. Abramova, and P. Keim.** 1998. PCR analysis of tissue samples from the 1979 Sverdlovsk anthrax victims: the presence of multiple *Bacillus anthracis* strains in different victims. Proc. Natl. Acad. Sci. USA **95**:1224–1229.
5. **Keim, P., A. Kalif, J. Schupp, K. Hill, S. E. Travis, K. Richmond, D. M. Adair, M. Hugh-Jones, C. R. Kuske, and P. Jackson.** 1997. Molecular evolution and diversity in *Bacillus anthracis* as detected by amplified fragment length polymorphism markers. J. Bacteriol. **179**:818–824.
6. **Leppla, S. H.** 1982. Anthrax toxin edema factor: a bacterial adenylate cyclase that increases cyclic AMP concentrations of eukaryotic cells. Proc. Natl. Acad. Sci. USA **79**:3162–3166.
7. **Li, W., and D. Graur.** 1991. Fundamentals of molecular evolution. Sinauer Associates, Inc., Sunderland, Mass.
8. **Little, S. F., J. M. Novak, J. R. Lowe, S. H. Leppla, Y. Singh, K. R. Klimpel, B. C. Ligerding, and A. M. Friedlander.** 1996. Characterization of lethal factor binding and cell receptor binding domains of protective antigen of *Bacillus anthracis* using monoclonal antibodies. Microbiology **142**:707–715.
9. **Perelle, S., M. Gibert, P. Boquet, and M. R. Popoff.** 1993. Characterization of *Clostridium perfringens* iota-toxin genes and expression in *Escherichia coli*. Infect. Immun. **61**:5147–5156.
10. **Petosa, C., R. J. Collier, K. R. Klimpel, S. H. Leppla, and R. C. Liddington.** 1997. Crystal structure of the anthrax toxin protective antigen. Nature **385**: 833–838.
11. **Selvapandiyan, A.** 1998. Direct submission. Genbank accession no. Y17158.
12. **Welkos, S. L., J. R. Lowe, F. Eden-McCutchan, M. Vodkin, S. H. Leppla, and J. J. Schmidt.** 1988. Sequence and analysis of the DNA encoding protective antigen of *Bacillus anthracis*. Gene **69**:287–300.

INFECTION AND IMMUNITY, Apr. 1999, p. 1860–1865
0019-9567/99/$04.00+0

Vol. 67, No. 4

Identification of a Receptor-Binding Region within Domain 4 of the Protective Antigen Component of Anthrax Toxin

MINI VARUGHESE, AVELINO V. TEIXEIRA,† SHIHUI LIU, AND STEPHEN H. LEPPLA*

Oral Infection and Immunity Branch, National Institute of Dental and Craniofacial Research, National Institutes of Health, Bethesda, Maryland 20892

Received 10 November 1998/Returned for modification 9 December 1998/Accepted 14 January 1999

Anthrax toxin from *Bacillus anthracis* is a three-component toxin consisting of lethal factor (LF), edema factor (EF), and protective antigen (PA). LF and EF are the catalytic components of the toxin, whereas PA is the receptor-binding component. To identify residues of PA that are involved in interaction with the cellular receptor, two solvent-exposed loops of domain 4 of PA (amino acids [aa] 679 to 693 and 704 to 723) were mutagenized, and the altered proteins purified and tested for toxicity in the presence of LF. In addition to the intended substitutions, novel mutations were introduced by errors that occurred during PCR. Substitutions within the large loop (aa 704 to 723) had no effect on PA activity. A mutated protein, LST-35, with three substitutions in the small loop (aa 679 to 693), bound weakly to the receptor and was nontoxic. A mutated protein, LST-8, with changes in three separate regions did not bind to receptor and was nontoxic. Toxicity was greatly decreased by truncation of the C-terminal 3 to 5 aa, but not by their substitution with nonnative residues or the extension of the terminus with nonnative sequences. Comparison of the 28 mutant proteins described here showed that the large loop (aa 704 to 722) is not involved in receptor binding, whereas residues in and near the small loop (aa 679 to 693) play an important role in receptor interaction. Other regions of domain 4, in particular residues at the extreme C terminus, appear to play a role in stabilizing a conformation needed for receptor-binding activity.

Anthrax toxin, a three-part toxin from *Bacillus anthracis*, consists of protective antigen (PA), lethal factor (LF), and edema factor (EF) (32). PA, the receptor-binding component of the toxin, binds to an unidentified receptor. PA is cleaved by a furin-like protease (14) and undergoes receptor-mediated endocytosis (8, 10). The PA oligomerizes to form a pore-like heptameric structure (15, 21) and transfers LF and EF into the cytosol, where LF and EF induce cytotoxic events (15, 16). The combination of LF and PA, known as lethal toxin (LT), lyses mouse macrophages within 90 min after addition of the toxin (8, 11). LF is a zinc metalloprotease (13) that is known to cleave at least two targets, mitogen-activated protein kinase kinases 1 and 2 (MAPKK1 and MAPPK2) (4, 35). Cleavage of MAPKK1 by LF inactivates MAPKK1.

Previous research localized the receptor-binding domain of the 735-amino-acid PA to the C terminus, within domain 4 (amino acids [aa] 596 to 735). Comparison of the amino acid sequence of PA with those of iota-*b* toxin from *Clostridium perfringens* (23) and the vegetative insecticidal proteins from *Bacillus cereus* and *Bacillus thuringiensis* (36) shows that these toxins have a high degree of similarity except in the C-terminal domains (24). Two monoclonal antibodies, 3B6 and 14B7 (17), recognize the region between aa 671 and 721 (18) and block the ability of PA to bind to its receptor, thereby protecting murine macrophage J774A.1 cells from PA-plus-LF challenge. In addition, C-terminal truncations of PA by 3 to 7 aa reduce the toxicity of PA plus LF, due to decreased ability of PA to bind to its receptor (30). Direct evidence that domain 4 contains the receptor recognition site is the demonstration that a CNBr fragment of PA, aa 663 to 735, is able to compete with PA for binding to cells (22).

To produce therapeutic agents, vaccines, and cell biology reagents derived from the anthrax toxin components (9), it would be advantageous to direct PA toward specific types of cell surface receptors. Because the PA receptor is present on most cell types, specificity would be improved if these reagents were derived from a mutant PA protein that is unable to bind to its own receptor. A fusion protein of wild-type PA and the $p62^{c\text{-}Myc}$ epitope that is recognized by the antibody produced by the hybridoma cell line 9E10 showed that PA can be redirected to an alternate receptor (34). However, this fusion protein was still able to bind to the PA receptor. To determine which residues in domain 4 are involved in receptor interaction, two solvent-exposed, flexible loops of domain 4 were mutagenized by PCR to introduce alanine (Ala) substitutions. These loops lie between β strands $4\beta_8$ and $4\beta_9$ (aa 679 to 693) and between β strands $4\beta_9$ and $4\beta_{10}$ (aa 704 to 723) and are called the small and large loops, respectively (24). The resulting proteins were tested for PA receptor interaction by cytotoxicity and competitive binding assays. More than 50 mutant proteins were screened, and more than 25 were analyzed in detail. During synthesis of the PCR products, errors in PCR priming and extension produced novel mutations in domain 4, including unique C-terminal truncations. These mutagenized proteins were also tested for receptor interaction. Analysis of the resulting proteins showed that the native amino acids in the large loop and the last eight amino acids of PA are not essential for receptor specificity. C-terminally truncated proteins showed a decrease in toxicity, perhaps due to destabilization of domain 4. Most importantly, we identified several nontoxic mutants which implicate the small loop in receptor recognition.

* Corresponding author. Mailing address: Oral Infection and Immunity Branch, National Institute of Dental and Craniofacial Research, Bldg. 30, Room 316, 30 Convent Dr. MSC 4350, Bethesda, MD 20892-4350. Phone: (301) 594-2865. Fax: (301) 402-0396. E-mail: leppla@nih.gov.

† Present address: Division of Nephrology, Mount Sinai School of Medicine, New York, NY 10029-6574.

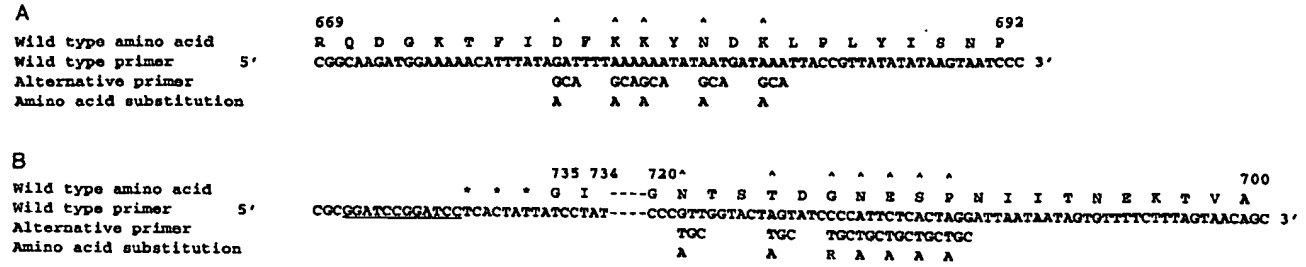

FIG. 1. PCR mutagenesis of PA. (A and B) Degenerate primers for PCR amplification of pYS5. The wild-type amino acid and nucleotide sequences (37) are shown below the amino acid residue numbers for PA. The nucleotide substitutions encoded by the degenerate primers are shown below the wild-type sequence along with the resulting amino acid substitutions. Carats indicate the sites at which, during the synthesis of the oligonucleotide chain, the synthesis was paused to permit mixing of the resin before synthesis of the next codon. Asterisks indicate stop codons, and the underlined nucleotides are two *Bam*HI restriction sites. (A) 5' 72-nt degenerate primer used for the first round of PCR to generate substitutions in the small loop of domain 4 of PA; (B) 3' 131-nt degenerate primer used to generate substitutions in the large loop of domain 4 of PA. The (unaltered) sequence at aa 733 to 721 is not shown so as to decrease the size of the figure.

MATERIALS AND METHODS

Reagents and supplies. Enzymes for DNA manipulation and modification were purchased from New England Biolabs, Inc. (Beverly, Mass.), Boehringer Mannheim (Indianapolis, Ind.), and Amersham Life Sciences (Arlington Heights, Ill.). Chemicals for protein work were purchased from Sigma (St. Louis, Mo.). Tissue culture products were purchased from Biofluids (Rockville, Md.) or Life Technologies (Grand Island, N.Y.), and the bacterial culture medium was purchased from Difco Laboratories (Detroit, Mich.).

Mutagenesis of PA domain 4 exposed loops. The codon-based mutagenesis protocol (3) used for mutagenesis of residues D677, K679, K680, N682, and K684 in the small loop of domain 4 required PCR amplification of the region R669 to G735 with a 3' wild-type primer and a mutagenic, degenerate 5' primer (Fig. 1A). The wild-type 3' primer 5'-CGCGGATCCGGATCCTCACTATTATCCTATC TCATAGCC-3' coded for residues G731 to G735 and two stop codons (TAG and TGA) in addition to the one TAA that exists at the 3' end of PA in pYS5. A double *Bam*HI restriction site and an appropriate clamp region for the *Bam*HI enzyme were added to the primer to allow for eventual cloning of the PCR product. The 5' degenerate 72-nucleotide (nt) primer (Fig. 1A) was synthesized on an Applied Biosystems (Foster City, Calif.) PCR-Mate 391 DNA synthesizer. During synthesis of the mutagenic primer, at positions where Ala substitutions were to be introduced, half of the resin from the 0.2-μmol DNA synthesis column was removed from the column. The Ala codon sequence, GCA (or the reverse complement, TGC), was synthesized on the remaining resin. The resin that was removed was placed into an empty column, and the wild-type codon sequence was synthesized on this column. The two resins were recombined, and synthesis of the primer continued until another Ala substitution site was reached, at which point the resin was again split. This splitting and mixing of resins created a mutagenic primer having 50% each of wild-type and Ala codons at the selected sites (Fig. 1A). When synthesis was completed, the oligonucleotide was removed from the resin according to standard protocols.

The wild-type 3' primer and the degenerate 5' primer were used to PCR amplify pYS5 (28) with the DNA polymerase *Taq* (Boehringer Mannheim). The pYS5 plasmid, encoding *pag* (37), the gene for PA, is an *Escherichia coli-Bacillus* shuttle vector. The PCR product generated from the pYS5 amplification was gel purified and fused by overlap PCR to a PCR product encoding PA S319 to I676. The DNA fragment encoding PA S319 to I676 was generated by PCR using the 5' primer 5'-AGTGTATCTGCAGGATTTAG-3 and 3' primer 5'-TATAAAT GTTTTTCCATCTTGCCG-3'. The 5' primer binds at the unique *Pst*I site in PA, and the 3' primer binds to the DNA region of PA at R669 to I676. The PCR product of PA R669 to I676 overlaps with the 5' end of the first PCR product created with the degenerate 5' and wild-type 3' primers, thereby permitting overlap PCR. The overlap PCR of the two PCR products was generated by using the *Pst*I primer as the 5' primer and the wild-type primer with the *Bam*HI recognition sites from the first PCR as the 3' primer. Thus, the PCR products had a *Pst*I site at the 5' end and a *Bam*HI site at the other end. A *Pst*I/*Bam*HI digest of the overlap PCR product was cloned between the *Pst*I and *Bam*HI sites of pYS5. The resulting clones were identified with the prefix LST.

A protocol similar to that described above was used for mutagenesis of residues P710, S711, E712, N713, G714, T716, and N719 in the large loop of domain 4 between β strands $4\beta_9$ and $4\beta_{10}$ of PA. The region of DNA from P710 to G735 was amplified with a 5' wild-type primer and degenerate 3' primer (Fig. 1B). The last step during the synthesis of the degenerate primer also added two stop codons and two *Bam*HI recognition sites at the end of the sequence, similar to the 3' wild-type primer prepared for the PCR of the small loop described above. The 5' primer overlapping the *Pst*I site, identical to the *Pst*I primer for the overlap PCR described above, and the degenerate 3' primer with the *Bam*HI site were used to PCR amplify pYS5. Gel-purified PCR product was digested with *Pst*I and *Bam*HI and ligated into *Pst*I/*Bam*HI-digested pYS5. The clones resulting from this procedure were also identified with the prefix LST. The region of *pag* between the *Pst*I and *Bam*HI sites of all LST plasmids was sequenced on both strands.

Mutagenesis of the C terminus of PA. The mutant PA LST8-min was created by site-directed mutagenesis of the C terminus of pYS5 with a QuickChange site-directed mutagenesis kit (Stratagene, La Jolla, Calif.). PA LST8-MV was created by site-directed mutagenesis of pYS5 by modification of the ExSite PCR-based site-directed mutagenesis protocol (Stratagene). LA Taq (TaKaRa Biochemical Inc., Berkeley, Calif.) was used instead of the supplied polymerase for the ExSite reaction. LST-51L was created by PCR amplification of pPA26 (37), which encodes PA. A 5' wild-type primer and a 3' mutagenic primer and *Pfu* polymerase were used to amplify the regions that overlapped the *Hin*dIII/*Sma*I sites of pPA26. The *Hin*dIII site is within and near the 5' end of the coding region for *pag*. The *Sma*I site on pPA26 lies beyond the 3' coding region of *pag*. The 3' mutagenic primer was engineered to encode a *Bam*HI site for future manipulation, which introduced an extra serine at the C terminus of PA. The PCR product was digested with *Hin*dIII and *Sma*I and cloned into the *Hin*dIII/*Sma*I site of pYS5. DNA isolated from the transformations for pLST8-min, pLST8-MV, and LST-51L were sequenced and then used for further experiments.

Expression and purification of protein. To express the mutagenized proteins, the plasmids were first transformed into the *E. coli dcm dam* strain GM2163. The unmethylated GM2163 DNA was then transformed into *B. anthracis* UM23C1-1 (25), from which the secreted protein was isolated as a crude preparation, as described previously (34). Culture supernatants were made to 5 mM EDTA and 35% saturation of ammonium sulfate (200 g added to each liter of supernatant), and 10 ml of phenyl-Sepharose Fast Flow (Pharmacia) was added per liter. After gentle agitation for 60 min, the resin was collected on a filter, washed with 35% saturated ammonium sulfate, and eluted with 10 mM HEPES–1 mM EDTA (pH 7.5). The resulting preparations were more than 50% pure. The LST-8, LST-26, and LST-35 proteins were further purified on a 1-ml MonoQ column (Pharmacia Biotech), using a 30 to 200 mM NaCl gradient in 10 mM CHES (2-[*N*-cyclohexylamino]ethanesulfonic acid)–0.06% (vol/vol) ethanolamine (pH 9.1). The pooled MonoQ fractions were dialyzed against 10 mM HEPES–1 mM EDTA (pH 8.0), concentrated with a Centricon 50 (Amicon, Beverly, Mass.), and analyzed by native 8 to 25% Phast gel electrophoresis (Pharmacia Biotech).

LST8-MV was isolated from the media of *B. anthracis* cultures grown in the presence of 3% horse serum to limit proteolysis, using an immunoadsorbent made from monoclonal anti-PA antibody 10G4 (17) as previously described for other PA mutants (30). The 10G4 immunoglobulin G was isolated from ascites fluid by using a MabTrapG kit (Pharmacia Biotech), and the purified 10G4 was then coupled to activated CNBr-Sepharose (Pharmacia Biotech). The 10G4-coupled resin was added to the *B. anthracis* culture supernatant, and the protein was eluted from the resin with 2 M NaSCN–20 mM HEPES–1 mM EDTA (pH 7.5). After extensive dialysis against 20 mM HEPES–1 mM EDTA (pH 7.5), the protein was concentrated with a Centricon 50 (Amicon) and analyzed by sodium dodecyl sulfate-polyacrylamide gel electrophoresis on 8 to 25% gradient gels (Phast gels; Pharmacia Biotech).

Quantitation of protein. For crude extracts, the amount of the mutated PA protein was determined with the Mancini radial diffusion assay (20). Briefly, a goat antiserum against PA was added to agarose medium to create antibody-impregnated plates. Holes were punched in the agarose gel, and samples were added. After incubation at 37°C for 1 to 3 days, the concentrations of the mutagenized proteins were determined by comparison of the diameters of the immunoprecipitation rings to a standard curve prepared from purified PA.

Cell culture. RAW264.7 cells (mouse macrophages) were cultured in Dulbecco's modified Eagle's medium with 4,500 mg of D-glucose per liter, 10% (vol/vol) fetal bovine serum, 50 μg of gentamicin per ml, 10 mM HEPES, and 2 mM glutamine.

Cytotoxicity assays. The macrophage lysis assay was used to measure the toxicity of the mutagenized PA proteins for RAW264.7 macrophages (26). PA, as

PA protein	651 β6	661 β7	671 β8	681	691 β9	701	711	721 β10	731 α3	Toxicity
Wild type	GLKEVINDRY	DMLNISSLRQ	DGKTFIDFKK	YNDKLPLYIS	NPNYKVNVYA	VTKENTIINP	SENGDTSTNG	IKKILIPSKR	GYEIG*	++
(aa targeted)			A AA	A A		A	AAAA A A			
LST-8	------S---	----------	----------	----------	----------	----------	-RA--A--A-	----------	-R*	-
LST-15	----------	----------	----------	----------	----------	---------A	ARA--A----	----------	-----*	++
LST-26	----------	----------	----------	----------	----------	---------A	ARA--A----	----------	-*	+
LST-27	----------	----------	----------	----------	----------	---------A	A-AA-A--A-	----------	-----*	++
LST-41	----------	----------	----------	----------	----------	---------A	--AA------	------L--R	L*	++
LST-8MV	----------	----------	----------	----------	----------	----------	----------	----------	-R*	++
LST-8min	----------	----------	----------	----------	----------	----------	----------	----------	-RRSRGNSR*	++
LST-51L	----------	----------	----------	----------	----------	----------	----------	-------AAS	-AS--S*	++
LST-33	----------	----------	------A-AA	----------	----------	----------	----------	----------	-----*	++
LST-35	----------	----------	------T--A	-A--------	----------	----------	----------	----------	-----*	-
LST-9	----------	----------	----------	----------	----------	---------A	-R--------	----------	-----*	++
LST-12	----------	----------	----------	----------	----------	---------A	-RA--A----	----------	-----*	++
LST-13	----------	----------	----------	----------	----------	---------A	----------	----------	-----*	++
LST-16	----------	----------	----------	----------	----------	--------S-	-R---A--A-	----------	-----*	++
LST-17	----------	----------	----------	----------	----------	---------A	A---------	----------	-----*	++
LST-18	----------	----------	----------	----------	----------	--------S-	-R--ESRMP-	HT--------	-----*	++
LST-19	----------	----------	----------	----------	----------	----------	C---------	----------	-----*	++
LST-21	----------	----------	----------	----------	----------	----------	A---------	----------	-----*	++
LST-23	----------	----------	----------	----------	----------	---------A	-RA-------	----------	-----*	++
LST-24	----------	----------	----------	----------	----------	----------	-R-A------	----------	-----*	++
LST-25	----------	----------	----------	----------	----------	---------A	A-------A-	----------	-----*	++
LST-39	----------	----------	----------	----------	----------	---------A	A-A-------	----------	-----*	++
LST-40	----------	----------	----------	----------	----------	---------A	A-AA-A----	----------	-----*	++
LST-43	----------	----------	----------	----------	----------	----------	AR--------	----------	-----*	++
LST-44	----------	----------	----------	----------	----------	----------	-RA-----A-	----------	-----*	++
LST-45	----------	----------	----------	----------	----------	---K-----A	-RAA-A----	----------	-----*	++
LST-46	----------	----------	----------	----------	----------	----------	-----A--A-	----------	-----*	++
LST-47	----------	----------	----------	----------	----------	----------	-R---A--A-	----------	-----*	++

FIG. 2. Mutated PA protein sequences. Shown are the C-terminal amino acid sequences of mutated PA proteins from residue 651 to the end of the protein sequence (indicated by *). The β-strand (β) and α-helical (α) motifs of PA are indicated above the wild-type PA sequence (37) as determined from the PDB file of the crystal structure of PA (PDB ID code 1ACC) (24). The motifs are numbered according to their sequential appearance in domain 4 of PA. Regions targeted for mutagenesis included the small loop, aa 678 to 693, and the large loop, aa 704 to 723. The substituted amino acids are indicated in the sequence. Toxicities of the proteins as determined from RAW264.7 cell cytotoxicity assays are indicated at the column right as ++ (10 to 100% as toxic as wild type), + (2 to 10% as toxic as wild type), or − (<0.1% as toxic as wild type).

a control, or the mutagenized proteins were serially diluted in the presence of 100 ng of LF per ml. The protein solution was added to one-third confluent, adherent RAW264.7 cells in a 96-well microtiter plate to a final volume of 200 μl/well. The cells were incubated for 3 h at 37°C in the presence of toxin. Cell viability was assayed by adding MTT (3-[4,5-dimethylthiazol-2-yl]-2,5-diphenyltetrazolium bromide), which is converted by viable cells to an insoluble blue pigment, which was dissolved and measured as described previously (34).

Competitive cytotoxicity assays. For the competitive cytotoxicity assays, the mutagenized PA proteins at various fixed concentrations and 100 ng of LF per ml were first added to a microtiter dish. Then native PA was added and serially diluted in the wells, holding the concentration of the mutated PA and LF constant. For comparison to the mutant PA proteins, we used PA ΔFF, a nontoxic receptor-binding variant of PA in which residues F313 and F314 are deleted (29). The protein mixture was added to RAW264.7 cells, and the cytotoxicity assay was performed as detailed above. The EC_{50}s (concentrations of toxin required to kill 50% of the cells) from the competition assays were used to construct Schild plots (12).

RESULTS

Mutagenesis of domain 4 exposed loops of PA (LST clones). Although the crystal structure of PA was recently solved (24), little work has been done to identify residues in domain 4 that are involved in binding to receptor. Therefore, we chose a mutagenesis method that would economically survey many residues simultaneously. We targeted two loops on the domain 4 surface that is predicted from the structure of the heptameric PA63 to face toward the cell surface. These two loops are solvent exposed and differ most from the homologous region of *C. perfringens* iota toxin. Codon-based mutagenesis (3) permitted the creation of multiple substitutions in different combinations (Fig. 1A). Selection of residues to mutagenize was somewhat arbitrary, although hydrophilic residues that were more likely to be surface exposed were preferred. Because a convenient restriction site was not available between the *Pst*I and *Bam*HI restriction sites, mutagenesis of the 15-aa small loop between β strands $4\beta_8$ and $4\beta_9$ required overlap PCR with an upstream PCR-amplified product. Only two mutants were obtained from this mutagenesis reaction. The mutagenesis of the 20-aa large loop between β strands $4\beta_9$ and $4\beta_{10}$ was simpler, and over 40 mutants were isolated from the mutagenesis of this region. Some plasmids were also found to code for novel mutations not encoded by the primers.

Cytotoxicity of PA domain 4 mutants (LST clones). If a mutation in the PA prevents binding of the protein to the PA receptor, then the mutagenized PA (LST proteins) and LF should not be cytotoxic to RAW264.7 cells (mouse macrophages). Most of the mutant PA proteins were toxic when tested in the presence of LF (Fig. 2). All of the PA proteins with substitutions restricted to the large loop were fully toxic. For example, LST-18 had eight substitutions in the large loop (aa 709, 712, 715 to 719, and 721 to 722) and remained fully toxic. Only two of the LST clones, LST-35 and LST-8, were nontoxic (Fig. 3). LST-26 was partially toxic, with an EC_{50} of 1,000 ng/ml, compared to 60 ng/ml for PA (Fig. 3).

Role of C-terminal residues of PA. PCR amplification with *Taq* polymerase introduced novel mutations into the PA proteins (5, 31). The proteins LST-8, LST-26, and LST-41 were found to have C-terminal truncations. Analysis of these proteins showed that LST-8 was nontoxic, LST-26 was partially

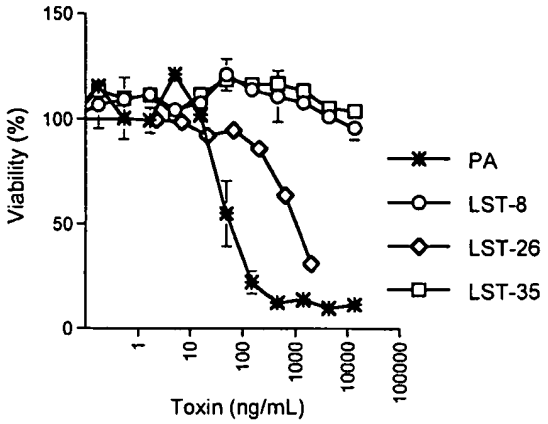

FIG. 3. Cytotoxicity assays. PA or the LST proteins were serially diluted into a 96-well plate containing RAW264.7 cells in the presence of LF (100 ng/ml). After 3 h of toxin challenge, MTT was added to determine cell viability. Data points are the mean ± standard deviation of triplicate wells, and the experiment shown is representative of the three performed.

toxic, and LST-41 was fully toxic in the presence of LF (Fig. 2). LST-26 has the same internal amino acid substitutions as the fully toxic mutant LST-15, suggesting that the truncation was responsible for the decreased activity of LST-26. However, LST-41 was similarly truncated and was fully toxic. Also, LST-8, which was nontoxic, has a novel mutation at the C terminus not present in LST-26, namely, a Y732R substitution. However, LST-8 also has an N657S substitution not found in any other protein.

To more closely examine the role of truncations and of the Y732R substitution, site-specific mutagenesis was used to construct two additional mutants, LST-8MV and LST-8min. Both LST-8MV and LST-8min have the Y732R substitution at the C terminus, similar to LST-8 (Fig. 2). LST-8MV has the same truncation as LST-8, whereas LST-8min has an extension of seven nonnative amino acids beyond the Y732R terminus of LST-8MV and LST-8. Both LST-8MV and LST-8min were found to be fully toxic. Then to test whether mutagenesis of the C-terminal residues to neutral residues would affect the toxicity and ability of PA to bind to its receptor, LST-51L was created. This protein, like LST-8MV and LST-8min, was fully toxic (Fig. 2).

Because LST-8 was nontoxic, competitive cytotoxicity assays were performed to determine if LST-8 bound to the PA receptor (Fig. 4A). If the LST protein does not compete with PA, then the LST protein is nontoxic because the protein is unable to bind to the receptor. In the presence of competitor, competition is shown by shifts of the cytotoxicity dose-response curve to the right. The nontoxic variant of PA, PA ΔFF, was used as a control (Fig. 4B). PA ΔFF is a variant of PA that binds to the receptor but is nontoxic because of a mutation that affects membrane channel formation and translocation (29). The data show that PA ΔFF protected the cells from PA (Fig. 4B) but that LST-8 did not (Fig. 4A). In fact, LST-8 was tested at concentrations up to 42 μg/ml and still failed to protect the cells from PA.

Role of small loop residues. Due to the complex nature of the PCR mutagenesis of the small loop (Fig. 1A), only two clones LST-33 and LST-35, were recovered from the mutagenesis of this region (Fig. 2). LST-33 was fully toxic, whereas LST-35 was nontoxic. LST-33 and LST-35 both contained substitutions at residues D677 and K680. N682 was the only residue of LST-35 not substituted in LST-33, suggesting that it may play a major role in receptor recognition. Competition assays were performed with LST-35 in the same way as for LST-8 (Fig. 4). The EC_{50} of each curve was then used in a Schild plot to calculate the K_d (dissociation constant). LST-35, which was at least 100-fold less toxic than wild native PA (Fig. 3), did bind to the PA receptor (Fig. 4C), although the K_d was only 4×10^{-8} M, compared with 6×10^{-9} M for PA ΔFF.

DISCUSSION

The intent of this research was to mutagenize the small and large solvent-exposed loops of domain 4 of PA (amino acids 679 to 693 and 704 to 723, respectively) to determine which residues in this region are involved in receptor interaction. Substitutions within the large loop had little or no effect on the ability of PA to kill RAW264.7 cells in the presence of LF (Fig. 2). These data show that the large loop probably does not interact directly with the receptor, and if it participates less directly in receptor interaction, this function is tolerant of many amino acid substitutions. Too few proteins mutated in the small loop were obtained to fully characterize the role of this loop in receptor interaction. However, the two proteins mutated in this region were informative because they differed substantially in activity, with LST-33 having normal activity and LST-35 being nontoxic. LST-35, even though nontoxic, was still capable of binding to the receptor, but with about 10-fold less affinity than PA (discussed below). The other nontoxic mutant obtained in this study, LST-8, has four substitutions in the large loop, but its lack of activity must be due to other mutations, as discussed below.

Some of the mutagenized plasmids obtained in this work were found to contain novel, unintended mutations, apparently introduced either by PCR or by the extensive manipulations of the PCR primers. Fortunately, several of these mutations helped to elucidate the function of the extreme C-terminal region of PA. One protein, LST-26, had an unexpected 4-aa C-terminal truncation and was partially toxic (Fig. 2 and 3). Comparison of LST-26 with LST-15 showed that the truncation in LST-26 was responsible for its decreased toxicity. The decreased activity of LST-26 is consistent with previous research which had shown that truncation of three, five, or seven residues from the C terminus reduces toxicity, while larger truncations of 12 or 14 aa abolishes toxicity of PA (30). However, LST-41 and LST8-MV were also truncated, and both were fully toxic (Fig. 2). These two proteins have additional mutations at the extreme C terminus that are not present in LST-26. These data indicate that while simple truncations of the C terminus generally reduce toxicity, extensive substitutions do not necessarily reduce toxicity. Substitution of native C-terminal residues with alternate residues may stabilize the structure of the protein compared to truncation of those residues. In particular, it appears that the Y732R substitution present in LST-8MV (and LST-8) may compensate for truncation of the proximal three amino acid residues. The crystal structure data show that the C terminus of PA is an α helix (24). This helix is the region that is truncated in LST-26, LST-41, and LST8-MV (Fig. 2). However, protein prediction programs such as PredictProtein (27) do not predict the helical motif observed by X-ray diffraction and cannot accurately predict whether substitutions in this region disrupt the helix.

Further evidence that the extreme C terminus is not critical to receptor binding is the somewhat surprising retention of activity in LST8-min and LST-51L, which have multiple substitutions at the extreme C terminus. Both of these proteins were fully toxic in the presence of LF. In fact, addition of an extra 16 aa to the C terminus of wild-type PA does not affect

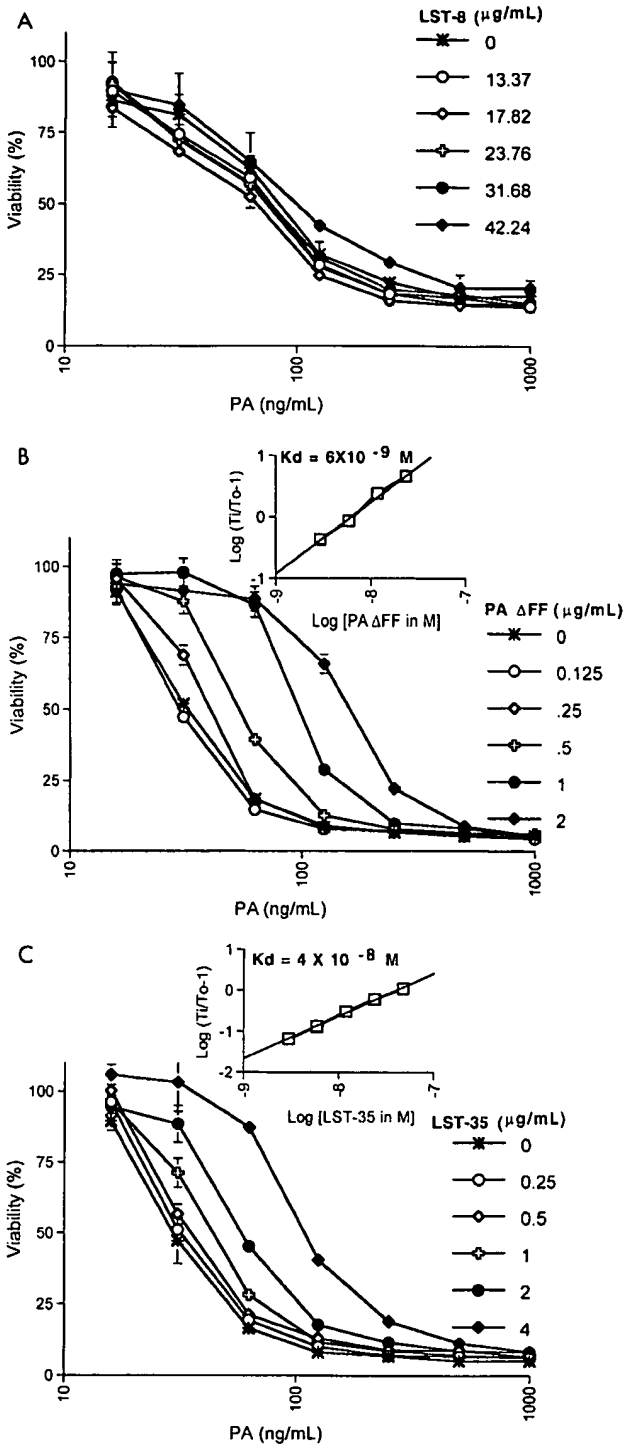

FIG. 4. Assay of mutated PA proteins for competitive inhibition of cytotoxicity. For the assay, LST-8 (A), PA ΔFF (B), or LST-35 (C) at various concentrations, in the presence of LF (100 ng/ml), was added to 96-well plates containing RAW264.7 cells. PA was serially diluted into the wells; after 3 h of toxin challenge, MTT was added to determine cell viability. Viability was normalized to wells lacking PA. The insets in panels B and C show the Schild plots and derived K_ds constructed from the EC_{50} values plotted on the graphs. The EC_{50}s for PA in the absence and presence of competitor are indicated as To and Ti, respectively. Data points are the mean ± standard deviation of triplicate wells, and the experiments shown are representative of the two to four that were performed for each mutant PA.

toxicity (34). This supports the view that the native residues at the C terminus of PA do not confer receptor specificity but instead stabilize the PA structure in a way that permits the protein to interact with the receptor.

For the two proteins found to be nontoxic, LST-8 and LST-35 (Fig. 3), competition assays showed that LST-8 does not bind to PA receptor, while LST-35 binds to the receptor with a decreased affinity (K_d of 4×10^{-8} M) (Fig. 4A and C). For comparison, PA ΔFF, a nontoxic but receptor-binding variant of PA, had a K_d of 6×10^{-9} M (Fig. 4B). The K_d of PA is 1×10^{-9} to 5×10^{-9} M (6, 30). Thus, LST-35 has 10- to 40-fold-lower affinity for the PA receptor. Because PA must form a heptamer as part of the intoxication process (15, 21), a 10-fold-lower affinity for receptor could cause a decrease in toxicity that is much greater than 10-fold, theoretically even approaching 10^7-fold. This may explain the lack of toxicity of LST-35.

The most informative and potentially useful mutants obtained in this study are LST-8 and LST-35. The nontoxic LST-8 protein has alterations in three regions. Comparison to the toxic mutant proteins discussed above shows that the substitutions in the large loop and at the C terminus of LST-8 are probably not responsible for its lack of toxicity, indicating that the N657S substitution may be the critical change. Comparison of the residues mutated in LST-35 with those in LST-33 suggests that the N682A substitution in LST-35 may be responsible for its lack of toxicity. It should be added that this type of argument does not consider the possibility that several substitutions or truncations which individually have no effect on toxicity can interact to disable the protein. This type of effect, if present, will probably become evident once a thorough analysis of individual local regions is completed.

The PA crystal structure (24) provides a possible explanation as to how the two critical residues identified by analysis of LST-8 and LST-35, namely, N657 and N682, might both be involved in receptor interaction. Although not adjacent in the primary sequence, the two residues are only 8 Å apart in the crystal structure. N657 is a partially buried residue, whereas N682 is surface exposed. The proximity of N657 and N682 suggests that Ala or possibly other substitutions at these positions alter the structure of the surface-exposed small loop area so as to decrease the affinity of PA for its receptor. This indicates that the essential receptor-binding residues may lie within or near the small loop. Consistent with this proposal, the X-ray crystal structure shows that the large loop and the C-terminal α helix of domain 4 lie on the opposite face of the protein from the small loop, consistent with their limited role in receptor binding as revealed by the large loop mutants.

Despite the fact that the majority of the clones isolated from the mutagenesis of PA were still toxic, the two nontoxic proteins, LST-35 and LST-8, and the truncation data indicate that domain 4 of PA is the receptor-binding domain. Domain 4 appears to be a separate domain and shows limited contact with the other three domains (24). Molecular modeling of the heptamer formed by PA during the intoxication process suggests that domain 4 swings out of the way during membrane insertion. Also, fusion of a $p62^{c\text{-}Myc}$ epitope to the C terminus of wild-type PA permits this fusion toxin to use antibody directed against the epitope as a receptor (34). Fusion of novel epitopes to LST-8, which does not bind PA receptor, should permit the creation of new anthrax toxins directed to specific cell types. An alternative strategy for redirecting PA would be to delete domain 4 and replace it with other receptor-binding domains. Other modular toxins, such as diphtheria toxin (1, 2, 7, 19) and *Pseudomonas* exotoxin (2, 33), have been modified to target new receptors. In fact, fusion of the Fc-binding do-

main of protein A to diphtheria toxin created a toxin that was more potent than the intact diphtheria toxin (19).

In conclusion, mutagenesis of the large loop (aa 704 to 722) in domain 4 of PA did not affect the ability of PA to bind receptor. Truncation of the C terminus, even of only 3 aa, reduced the ability of PA to bind to its receptor. In contrast, substitution of the last 8 aa had no effect on the toxicity of PA in conjunction with LF. This work has established that the native amino acid residues in the large loop of domain 4 and at the C terminus of PA are not essential for receptor binding, but instead an intact C-terminal structural motif seems necessary for toxicity and receptor interaction. The receptor binding residues of PA lie within domain 4, probably in the small loop between β strands $4\beta_8$ and $4\beta_9$. Analysis of the large number of mutants described here has succeeded in localizing a small region involved in receptor binding. Further work is in progress to delineate the roles of the individual residues in this region.

ACKNOWLEDGMENTS

We thank Carlo Petosa for helpful advice on targeted mutagenesis and Marian Betz and Ryan Miyamoto for technical assistance.

REFERENCES

1. **Aullo, P., J. Alcami, M. R. Popoff, D. R. Klatzmann, J. R. Murphy, and P. Boquet.** 1992. A recombinant diphtheria toxin related human CD4 fusion protein specifically kills HIV infected cells which express gp120 but selects fusion toxin resistant cells which carry HIV. EMBO J. **11**:575–583.
2. **Batra, J. K., D. J. FitzGerald, V. K. Chaudhary, and I. Pastan.** 1991. Single-chain immunotoxins directed at the human transferrin receptor containing *Pseudomonas* exotoxin A or diphtheria toxin: anti-TFR(Fv)-PE40 and DT388-anti-TFR(Fv). Mol. Cell. Biol. **11**:2200–2205.
3. **Cormack, B. P., and K. Struhl.** 1993. Regional codon randomization: defining a TATA-binding protein surface required for RNA polymerase III transcription. Science **262**:244–248.
4. **Duesbery, N. S., C. P. Webb, S. H. Leppla, V. M. Gordon, K. R. Klimpel, T. D. Copeland, N. G. Ahn, M. K. Oskarsson, K. Fukasawa, K. D. Paull, and G. F. Vande Woude.** 1998. Proteolytic inactivation of MAP-kinase-kinase by anthrax lethal factor. Science **280**:734–737.
5. **Eckert, K. A., and T. A. Kunkel.** 1991. DNA polymerase fidelity and the polymerase chain reaction. PCR Methods Appl. **1**:17–24.
6. **Escuyer, V., and R. J. Collier.** 1991. Anthrax protective antigen interacts with a specific receptor on the surface of CHO-K1 cells. Infect. Immun. **59**:3381–3386.
7. **Finberg, R. W., S. M. Wahl, J. B. Allen, G. Soman, T. B. Strom, J. R. Murphy, and J. C. Nichols.** 1991. Selective elimination of HIV-1-infected cells with an interleukin-2 receptor-specific cytotoxin. Science **252**:1703–1705.
8. **Friedlander, A. M.** 1986. Macrophages are sensitive to anthrax lethal toxin through an acid-dependent process. J. Biol. Chem. **261**:7123–7126.
9. **Goletz, T. J., K. R. Klimpel, N. Arora, S. H. Leppla, J. M. Keith, and J. A. Berzofsky.** 1997. Targeting HIV proteins to the major histocompatibility complex class I processing pathway with a novel gp120-anthrax toxin fusion protein. Proc. Natl. Acad. Sci. USA **94**:12059–12064.
10. **Gordon, V. M., S. H. Leppla, and E. L. Hewlett.** 1988. Inhibitors of receptor-mediated endocytosis block the entry of *Bacillus anthracis* adenylate cyclase toxin but not that of *Bordetella pertussis* adenylate cyclase toxin. Infect. Immun. **56**:1066–1069.
11. **Hanna, P. C., S. Kouchi, and R. J. Collier.** 1992. Biochemical and physiological changes induced by anthrax lethal toxin in J774 macrophage-like cells. Mol. Biol. Cell **3**:1269–1277.
12. **Ittelson, T. R., and D. M. Gill.** 1973. Diphtheria toxin: specific competition for cell receptors. Nature **242**:330–332.
13. **Klimpel, K. R., N. Arora, and S. H. Leppla.** 1994. Anthrax toxin lethal factor contains a zinc metalloprotease consensus sequence which is required for lethal toxin activity. Mol. Microbiol. **13**:1093–1100.
14. **Klimpel, K. R., S. S. Molloy, G. Thomas, and S. H. Leppla.** 1992. Anthrax toxin protective antigen is activated by a cell-surface protease with the sequence specificity and catalytic properties of furin. Proc. Natl. Acad. Sci. USA **89**:10277–10281.
15. **Leppla, S. H.** 1991. The anthrax toxin complex, p. 277–302. *In* J. E. Alouf and J. H. Freer (ed.), Sourcebook of bacterial protein toxins. Academic Press, London, England.
16. **Leppla, S. H.** 1995. Anthrax toxins. p. 543–572. *In* J. Moss, B. Iglewski, M. Vaughan, and A. Tu (ed.), Handbook of natural toxins. vol. 8. Bacterial toxins and virulence factors in disease. Marcel Dekker, Inc., New York, N.Y.
17. **Little, S. F., S. H. Leppla, and E. Cora.** 1988. Production and characterization of monoclonal antibodies to the protective antigen component of *Bacillus anthracis* toxin. Infect. Immun. **56**:1807–1813.
18. **Little, S. F., J. M. Novak, J. R. Lowe, S. H. Leppla, Y. Singh, K. R. Klimpel, B. C. Lidgerding, and A. M. Friedlander.** 1996. Characterization of lethal factor binding and cell receptor binding domains of protective antigen of *Bacillus anthracis* using monoclonal antibodies. Microbiology **142**:707–715.
19. **Madshus, I. H., H. Stenmark, K. Sandvig, and S. Olsnes.** 1991. Entry of diphtheria toxin-protein A chimeras into cells. J. Biol. Chem. **266**:17446–17453.
20. **Mancini, G., A. O. Carbonara, and J. F. Heremans.** 1965. Immunochemical quantitation of antigens by single radial immunodiffusion. Immunochemistry **2**:235–254.
21. **Milne, J. C., D. Furlong, P. C. Hanna, J. S. Wall, and R. J. Collier.** 1994. Anthrax protective antigen forms oligomers during intoxication of mammalian cells. J. Biol. Chem. **269**:20607–20612.
22. **Noskov, A. N., T. B. Kravchenko, and V. P. Noskova.** 1996. Detection of the functionally active domains in the molecule of protective antigen of the anthrax exotoxin. Mol. Gen. Mikrobiol. Virusol. **1996**:16–20. (In Russian.)
23. **Perelle, S., M. Gibert, P. Boquet, and M. R. Popoff.** 1993. Characterization of *Clostridium perfringens* iota-toxin genes and expression in *Escherichia coli*. Infect. Immun. **61**:5147–5156.
24. **Petosa, C., R. J. Collier, K. R. Klimpel, S. H. Leppla, and R. C. Liddington.** 1997. Crystal structure of the anthrax toxin protective antigen. Nature **385**: 833–838.
25. **Quinn, C. P., and B. N. Dancer.** 1990. Transformation of vegetative cells of *Bacillus anthracis* with plasmid DNA. J. Gen. Microbiol. **136**:1211–1215.
26. **Quinn, C. P., Y. Singh, K. R. Klimpel, and S. H. Leppla.** 1991. Functional mapping of anthrax toxin lethal factor by in-frame insertion mutagenesis. J. Biol. Chem. **266**:20124–20130.
27. **Rost, B.** PredictProtein. http://www.embl-heidelberg.de/Services/sander/predictprotein. [Online.] [29 January 1999, last date accessed.]
28. **Singh, Y., V. K. Chaudhary, and S. H. Leppla.** 1989. A deleted variant of *Bacillus anthracis* protective antigen is non-toxic and blocks anthrax toxin action in vivo. J. Biol. Chem. **264**:19103–19107.
29. **Singh, Y., K. R. Klimpel, N. Arora, M. Sharma, and S. H. Leppla.** 1994. the chymotrypsin-sensitive site, FFD315, in anthrax toxin protective antigen is required for translocation of lethal factor. J. Biol. Chem. **269**:29039–29046.
30. **Singh, Y., K. R. Klimpel, C. P. Quinn, V. K. Chaudhary, and S. H. Leppla.** 1991. The carboxyl-terminal end of protective antigen is required for receptor binding and anthrax toxin activity. J. Biol. Chem. **266**:15493–15497.
31. **Smedley, D. P., and D. J. Ellar.** 1996. Mutagenesis of three surface-exposed loops of a *Bacillus thuringiensis* insecticidal toxin reveals residues important for toxicity, receptor recognition and possibly membrane insertion. Microbiology **142**:1617–1624.
32. **Stanley, J. L., and H. Smith.** 1961. Purification of factor I and recognition of a third factor of anthrax toxin. J. Gen. Microbiol. **26**:49–66.
33. **Theuer, C. P., D. FitzGerald, and I. Pastan.** 1992. A recombinant form of *Pseudomonas* exotoxin directed at the epidermal growth factor receptor that is cytotoxic without requiring proteolytic processing. J. Biol. Chem. **267**: 16872–16877.
34. **Varughese, M., A. Chi, A. V. Teixeira, P. J. Nicholls, J. M. Keith, and S. H. Leppla.** 1998. Internalization of a *Bacillus anthracis* protective antigen c-Myc fusion protein mediated by cell surface anti-c-Myc antibodies. Mol. Med. **4**: 87–95.
35. **Vitale, G., R. Pellizzari, C. Recchi, G. Napolitani, M. Mock, and C. Montecucco.** 1998. Anthrax lethal factor cleaves the N-terminus of MAPKKs and induces tyrosine/threonine phosphorylation of MAPKs in cultured macrophages. Biochem. Biophys. Res. Commun. **248**:706–711.
36. **Warren, G. W., M. G. Koziel, M. A. Mullins, G. J. Nye, B. Carr, N. Desai, K. Kostischka, N. B. Duck, and J. J. Estruch.** 1996. Novel pesticidal proteins and strains. Patent application WO 96/10083 (1996). World Intellectual Patent Organization.
37. **Welkos, S. L., J. R. Lowe, F. Eden-McCutchan, M. Vodkin, S. H. Leppla, and J. J. Schmidt.** 1988. Sequence and analysis of the DNA encoding protective antigen of *Bacillus anthracis*. Gene **69**:287–300.

Editor: J. T. Barbieri

INFECTION AND IMMUNITY, Feb. 1999, p. 964–967
0019-9567/99/$04.00+0

Vol. 67, No. 2

Functional Analysis of the Carboxy-Terminal Domain of *Bacillus anthracis* Protective Antigen

FABIEN BROSSIER, JEAN-CLAUDE SIRARD, CHANTAL GUIDI-RONTANI, EDITH DUFLOT, AND MICHELE MOCK*

Unité Toxines et Pathogénie Bactériennes, Institut Pasteur, 75724 Paris Cedex 15, France

Received 3 September 1998/Returned for modification 10 November 1998/Accepted 30 November 1998

Protective antigen (PA) is the common receptor-binding component of the two anthrax toxins. We investigated the involvement of the PA carboxy-terminal domain in the interaction of the protein with cells. A deletion resulting in removal of the entire carboxy-terminal domain of PA (PA608) or part of an exposed loop of 19 amino acids (703 to 722) present within this domain was introduced into the *pag* gene. PA608 did not induce the lethal-factor (LF)-mediated cytotoxic effect on macrophages because it did not bind to the receptor. In contrast, PA711- and PA705-harboring lethal toxins (9- and 16-amino-acid deletions in the loop, starting after positions 711 and 705, respectively) were 10 times less cytotoxic than wild-type PA. After cleavage by trypsin, the mutant PA proteins formed heptamers and bound LF. The capacity of PA711 and PA705 to interact with cells was 1/10 that of wild-type PA. In conclusion, truncation of the carboxy-terminal domain or deletions in the exposed loop resulted in PA that was less cytotoxic or nontoxic because the mutated proteins did not efficiently bind to the receptor.

Bacillus anthracis, a spore-forming bacterium, is the causative agent of anthrax. The two exotoxins are main virulence factors of the microorganism. These toxins are composed of three proteins: the protective antigen (PA, 83 kDa), the lethal factor (LF, 85 kDa), and the edema factor (EF, 89 kDa) (7, 15). Intravenous injection of the lethal toxin (PA plus LF) causes sudden death in animals (1). The edema toxin (PA plus EF) causes edema at the inoculation site (29). The components PA, LF, and EF are encoded by the *pag*, *lef*, and *cya* genes, respectively, and these genes are carried by virulence plasmid pXO1 (185 kbp) (3, 17, 20, 32). A mode of action has been proposed for anthrax toxins (13). PA binds to a ubiquitous proteinaceous cell receptor which has yet to be identified (6). It is then cleaved by a furin-like protease into PA63 and PA20 (a 20-kDa amino-terminal fragment) (11, 26). This processing facilitates the heptamerization of PA63 (19) and the subsequent binding of EF or LF. These toxic complexes are internalized by receptor-mediated endocytosis. The pH within the acidic vesicles decreases during intracellular trafficking, resulting in the insertion of PA into the membrane and the formation of a channel (2, 12, 18). EF and LF are further translocated into the cytoplasm to exert their catalytic effects. EF is a calmodulin-dependent adenylate cyclase (14). LF is a zinc metalloprotease which cleaves mitogen-activated protein kinase kinases 1 and 2 (5, 10, 31). The lethal toxin induces the lysis of macrophage cell lines such as RAW264.7 (8). PA is therefore a key protein, promoting both the binding of the toxins and the translocation of their enzymatic moieties (27, 33). Previous studies have suggested that the carboxy-terminal extremity of PA is involved in the recognition of the cell receptor (16, 28). The three-dimensional structure of the monomeric PA has been solved at 2.1 Å resolution (21) and consists of four folding domains. Domain 4 of PA encompasses the last 139 carboxy-terminal amino acids (596 to 735). We analyzed the function of domain 4 in toxicity by constructing various deletions in the *pag* gene, based on the structural organization of the molecule. The cytotoxicity of the resulting protein products in the presence of LF and their interaction with the receptor were tested.

Construction of carboxy-terminal domain mutant PA. Domain 4 of PA contains an exposed loop of 19 amino acids which begins at position 703. Mutations affecting the whole of domain 4 of PA or the exposed loop were produced (Fig. 1). We thereby created stop codons after the sequences encoding arginine 592 (PA592) or aspartate 608 (PA608), removing the whole of domain 4 (PA592) or retaining the first 16 amino acids of this domain (PA608). Two short, in-frame deletions resulting in the removal of 9 (PA711) or 16 (PA705) amino acids from the loop were created after the nucleotides encoding residues 711 and 705, respectively. Mutants PA proteins were obtained by site-directed mutagenesis with a PCR. Plasmid pACP41 was used as the template for the PCR (23). The divergent sequences of the primers used were 5′-AAGAAAA TTTTAATCTTTTCTAAAAAAGGC-3′ and 5′-GTTTTCTT TAGTAACAGCATATACATTTAC-3′ for PA705, 5′-ACTA GGATTAATAATAGTGTTTTCTTTAG-3′ and 5′-ATCAA GAAAATTTTAATCTTTTCTAAAAAAGGC-3′ for PA711, and 5′-CTCACTAATCCGCCCCAACTGCTATG-3′ and 5′-GGCTATGAGATAGGATAAGGTAATTCT-3′ for PA608. For the construction of PA592, a stop codon was introduced by using a site-directed mutagenesis kit (Stratagene, La Jolla, Calif.). The mutated *pag* genes, cloned into shuttle plasmid pAT28 (30), were transferred by heterogramic mating as previously described (22) into PA-deficient *B. anthracis* RP31 (23), and the production of PA-related proteins was tested. The three mutated proteins, PA608, PA705, and PA711, were purified by fast protein liquid chromatography as previously described (23) from the supernatants of *B. anthracis* transconjugants grown in R medium (24) containing tryptone (5 g/liter). The molecular masses of the corresponding proteins were as expected (approximately 83 kDa for PA711 and PA705 and 70 kDa for PA608) (Fig. 2). In contrast, PA592 was not found in the supernatants of *B. anthracis*, suggesting that the amino acids between asparagine 592 and aspartate 608 are required for stability of the molecule.

* Corresponding author. Mailing address: Unité Toxines et Pathogénie Bactériennes (URA 1858, CNRS), Institut Pasteur, 28, rue du Dr. Roux, 75724 Paris Cedex 15, France. Phone: (33) 1.45.68.83.12. Fax: (33) 1.45.68.89.54. E-mail: mmock@pasteur.fr.

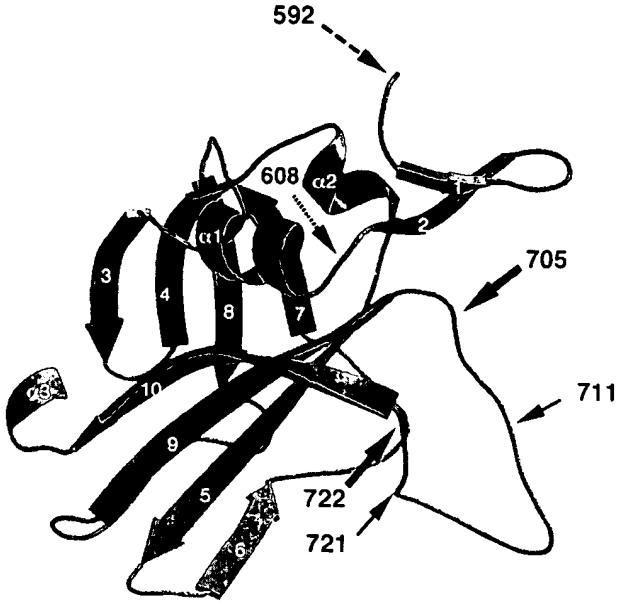

FIG. 1. Schematic representation of the mutagenesis of domain 4 of PA. The three-dimensional structure of the carboxy-terminal domain of PA (amino acids 592 to 735), according to Petosa et al. (21), is shown. We truncated the PA molecule by introducing a stop codon after the codon encoding arginine 592 or aspartate 608. Two in-frame deletions resulting in the removal of 9 and 16 amino acids (residues 711 to 721 and 705 to 722, respectively) were also created in the exposed loop of 19 amino acids (residues 703 to 722). Point mutations are indicated by dashed arrows; deletions are indicated by plain arrows.

Cytotoxicity of mutant PA in the presence of LF. We tested the ability of PA mutant proteins to induce LF-mediated lysis of murine macrophage cell line RAW264.7 (Fig. 3). A 20-ng/ml concentration of wild-type PA was required for lysis of half of the macrophages (50% effective concentration [EC_{50}]). PA608 was completely inactive against macrophages (EC_{50}, $>2 \times 10^4$ ng/ml). PA711 and PA705 were mildly toxic, with EC_{50}s of 2×10^2 and 6×10^2 ng/ml, respectively (EC_{50} of PA, 20 ng/ml). To determine which step of the intoxication process was affected,

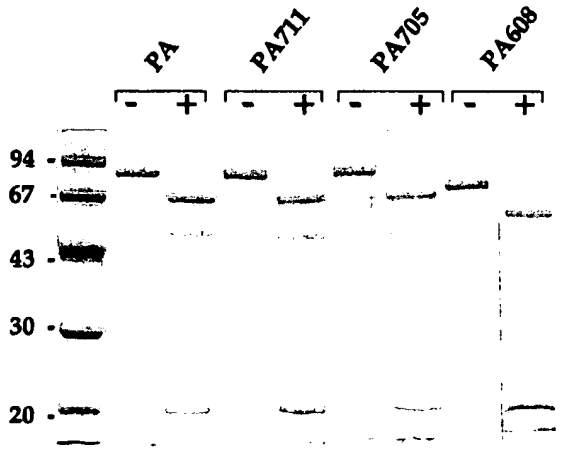

FIG. 2. Trypsin treatment of mutant PA. Wild-type and mutant PA proteins were purified from *B. anthracis* supernatants and studied in native form (−) or after (+) cleavage by trypsin. Samples (2 μg) were subjected to electrophoresis in a sodium dodecyl sulfate–12% polyacrylamide gel and stained with Coomassie blue. The values on the left are molecular masses in kilodaltons.

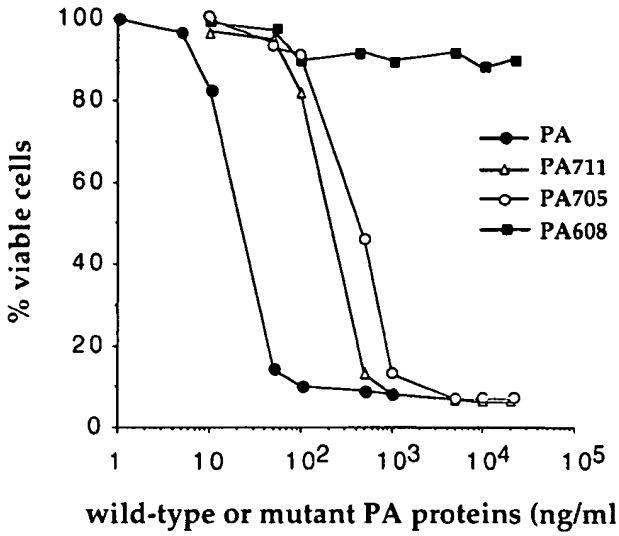

FIG. 3. Cytotoxicity assay for mutant PA. Wild-type or mutated PA protein (from $1 \times 2 \times 10^4$ to 2×10^4 ng/ml) was serially diluted into a 96-well plate containing RAW264.7 cells in the presence of a constant concentration of LF (2×10^4 ng/ml). The cells were incubated for 3 h, and their viability was assessed by using a 3-(4,5-dimethylthiazol-2-yl)-2,5-diphenyltetrazolium bromide assay (9). The experiment was carried out at least three times for each mutant PA protein.

we analyzed the interaction of the mutant PA with LF and with the cell receptor.

Interaction of mutant PA with LF. The interaction between PA and LF requires the proteolytic processing of PA by the furin-like protease. In vitro, trypsin mimics this action, cleaving PA into PA20 and PA63. Treatment of PA705, PA711, and PA608 with trypsin (600:1) for 30 min at 30°C released PA20 and a PA63 mutant polypeptide of the expected size (Fig. 2). Thus, the trypsin-sensitive site was exposed in the mutant molecules. Moreover, PA705 and PA711 formed heptamers after processing, as previously observed for wild-type PA (19) (data not shown). An assay was developed to detect the binding of LF to the mutant PA molecules. Purified LF protein (1 μg per well) was subjected to electrophoresis in a nondenaturing polyacrylamide gel and transferred to a nitrocellulose membrane (Hybond-C; Amersham, Buckinghamshire, England). Wild-type or mutated PA proteins (2 μg/ml), freshly treated with trypsin, were incubated with the LF blots for 16 h at 4°C. The PA63-LF complex was detected by Western blotting using rabbit anti-PA serum, followed by the addition of goat anti-immunoglobulin G coupled to peroxidase (ECL kit; Amersham). Only the trypsin-treated forms of the PA proteins recognized LF on the membrane (Fig. 4). A double signal was routinely observed which corresponded to the two isoforms of LF. The three mutant proteins interacted with LF in a manner similar to that of wild-type PA. Thus, (i) the conformation of the LF-binding region of PA was not significantly changed and (ii) domain 4 of PA was not required for the binding of LF, consistent with previous reports (16, 28).

Binding of mutant PA to cells. The binding of wild-type and mutant PA proteins to cells was tested on CHO-K1 cells, each of which has approximately 10,000 PA receptor molecules on its surface (6). An enzyme-linked immunosorbent assay was used to determine protein binding. The CHO-K1 cell line was seeded into 24-well plates (Costar) containing glass slides at a density of approximately 10^5 cells per well. The cells were incubated for 16 h at 37°C in a 5% CO_2–95% air atmosphere,

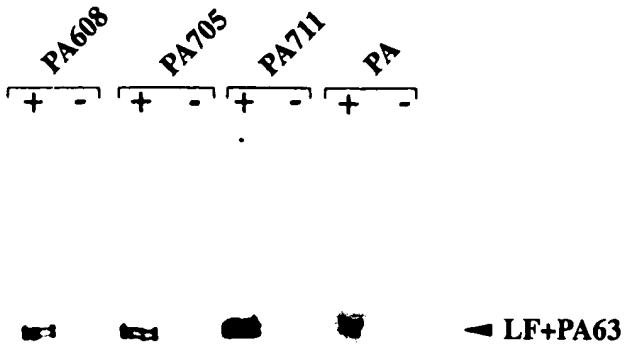

FIG. 4. Interaction of mutant PA proteins with LF. Purified LF protein was subjected to electrophoresis in a 10% nondenaturing polyacrylamide gel and transferred to a nitrocellulose membrane under nondenaturing conditions. Wild-type or mutated PA proteins (2 μg), untreated (−) or treated (+) with trypsin, were added. The filter was incubated for 16 h at 4°C, and the LF-PA63 complex was detected with anti-PA serum.

cooled for 15 min at 4°C, washed with cold phosphate-buffered saline (PBS), and incubated for 3 h at 4°C in RPMI 1640 with wild-type or mutant PA protein. Unbound proteins were removed by washing the cells with cold PBS. Cells were then fixed and then incubated with anti-PA serum (1/4,000) for 45 min at 37°C in PBS-skim milk powder (2%). After washing, goat anti-immunoglobulin G coupled to β-galactosidase (1/10,000) was added and incubated with cells in PBS-skim milk powder (2%) for 45 min at 37°C. The glass slides were washed with PBS and incubated for 30 min at 37°C with methylumbelliferyl-β-galactoside (MUG). The enzymatic reaction was stopped by addition of 100 mM glycine (pH 10.4). The hydrolysis of MUG by the β-galactosidase resulted in the formation of a fluorescent component. The level of fluorescence associated with cells was assessed on a fluoroscan fluorimeter (Titertek-Fluoroskan, Labsystem).

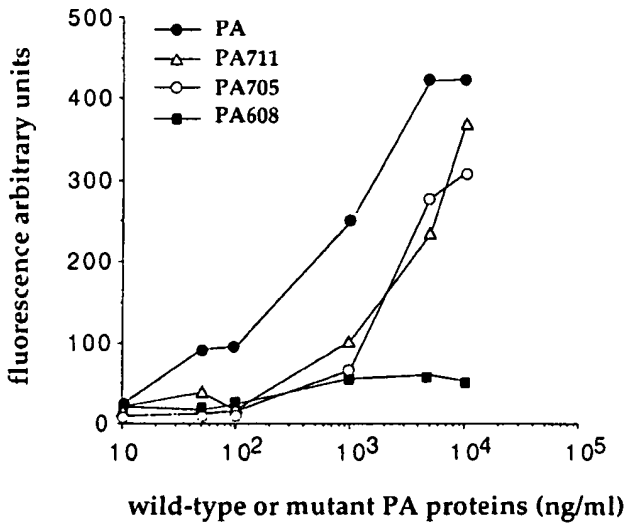

FIG. 5. Assay of binding of wild-type or mutant PA proteins to CHO-K1 cells. Various concentrations of wild-type or mutant PA proteins (from 10 to 1 × 10^4 ng/ml) were incubated with CHO-K1 cells for 3 h at 4°C. The binding of PA proteins to cells was detected with anti-PA serum and a secondary antibody coupled to β-galactosidase. MUG was added as the substrate for β-galactosidase, and fluorescence was quantified with a fluorimeter. The experiment was carried out at least three times for each mutant PA protein.

The threshold for detection of wild-type PA was about 10 ng/ml, and the receptors were saturated at a concentration of 5 μg/ml (Fig. 5). The truncated protein, PA608, did not bind to cells, even at high concentrations (10^4 ng/ml), and the level of binding of PA711 and PA705 to cells was significantly lower (1/10) than that of the wild-type protein. Therefore, the low cytotoxicity of domain 4 mutant PA is due to a defect in the receptor interaction of these molecules. The 19-amino-acid loop of PA is structurally similar to the 15-amino-acid (from residue 516 to residue 530) exposed loop in the binding domain of the diphtheria toxin (4). Replacement of Lys 516 and Phe 530 with Ala results in mutant diphtheria toxins that are 22 and 10 times less cytotoxic than the wild-type protein, respectively, because the molecules do not efficiently bind to the receptor (25). The exposed loops of PA and the diphtheria toxin may have similar functions. They may be involved in stabilization of the toxin-receptor complex or may participate in receptor recognition.

We are grateful to Carlo Petosa for helpful discussions on the design of mutant PA proteins. We also thank Evelyne Tosi-Couture for the observations by electron microscopy and Guy Patra for helpful discussions on the purification of the mutant PA proteins.

This work was supported by DRET (94-118). F.B. was supported by the Ministère de l'Enseignement Supérieur et de la Recherche.

REFERENCES

1. **Beall, F. A., M. J. Taylor, and C. B. Thorne.** 1962. Rapid lethal effects in rats of a third component found upon fractionating the toxin of *Bacillus anthracis*. J. Bacteriol. **83**:1274–1280.
2. **Blaustein, R. O., T. M. Koehler, R. J. Collier, and A. Finkelstein.** 1989. Anthrax toxin: channel-forming activity of protective antigen in planar phospholipid bilayers. Proc. Natl. Acad. Sci. USA **86**:2209–2213.
3. **Bragg, T. S., and D. L. Robertson.** 1986. Nucleotide sequence and analysis of the lethal factor gene (*lef*) from *Bacillus anthracis*. Gene **81**:45–54.
4. **Choe, S., M. J. Bennett, G. Fujii, P. M. G. Curmi, K. A. Kantardjieff, R. J. Collier, and D. Eisenberg.** 1992. The crystal structure of diphtheria toxin. Nature **357**:216–222.
5. **Duesbery, N. S., C. P. Webb, S. H. Leppla, V. M. Gordon, K. R. Klimpel, T. D. Copeland, N. G. Ahn, M. K. Oskarsson, K. Fukasawa, K. D. Paull, and G. F. Vandewoude.** 1998. Proteolytic inactivation of map-kinase-kinase by anthrax lethal factor. Science **280**:734–737.
6. **Escuyer, V., and R. J. Collier.** 1991. Anthrax protective antigen interacts with a specific receptor on the surface of CHO-K1 cells. Infect. Immun. **59**:3381–3386.
7. **Fish, D. C., B. G. Mahlandt, J. P. Dobbs, and R. E. Lincoln.** 1968. Purification and properties of in vitro-produced anthrax toxin components. J. Bacteriol. **95**:907–918.
8. **Friedlander, A. M.** 1986. Macrophages are sensitive to anthrax lethal toxin through an acid-dependent process. J. Biol. Chem. **261**:7123–7126.
9. **Hansen, M. B., S. E. Nielsen, and K. Berg.** 1989. Re-examination and further development of a precise and rapid dye method for measuring cell growth/cell kill. J. Immunol. Methods **119**:203–210.
10. **Klimpel, K. R., N. Arora, and S. H. Leppla.** 1994. Anthrax toxin lethal factor contains a zinc metalloprotease consensus sequence which is required for lethal toxin activity. Mol. Microbiol. **13**:1093–1100.
11. **Klimpel, K. R., S. S. Molloy, G. Thomas, and S. H. Leppla.** 1992. Anthrax toxin protective antigen is activated by a cell surface protease with the sequence specificity and catalytic properties of furin. Proc. Natl. Acad. Sci. USA **89**:10277–10281.
12. **Koehler, T. M., and R. J. Collier.** 1991. Anthrax toxin protective antigen: low pH-induced hydrophobicity and channel formation in liposomes. Mol. Microbiol. **5**:1501–1506.
13. **Leppla, S. H.** 1991. The anthrax toxin complex, p. 277–302. *In* J. E. Alouf and J. H. Freer (ed.), Sourcebook of bacterial protein toxins, vol. 14. Academic Press, San Diego, Calif.
14. **Leppla, S. H.** 1982. Anthrax toxin edema factor: a bacterial adenylate cyclase that increases cyclic AMP concentrations in eukaryotic cells. Proc. Natl. Acad. Sci. USA **79**:3162–3166.
15. **Leppla, S. H.** 1988. Production and purification of anthrax toxin. Methods Enzymol. **165**:103–116.
16. **Little, S. F., J. M. Novak, J. R. Lowe, S. H. Leppla, Y. Singh, K. R. Klimpel, B. C. Lidgerding, and A. M. Friedlander.** 1996. Characterization of lethal factor binding and cell receptor binding domains of protective antigen of

Bacillus anthracis using monoclonal antibodies. Microbiology (Reading) **142:** 707–715.
17. **Mikesell, P., B. E. Ivins, J. D. Ristroph, and T. M. Dreier.** 1983. Evidence for plasmid-mediated toxin production in *Bacillus anthracis*. Infect. Immun. **39:** 371–376.
18. **Milne, J. C., and R. J. Collier.** 1993. pH-dependent permeabilization of the plasma membrane of mammalian cells by anthrax protective antigen. Mol. Microbiol. **10:**647–653.
19. **Milne, J. C., D. Furlong, P. C. Hanna, J. S. Wall, and R. J. Collier.** 1994. Anthrax protective antigen forms oligomers during intoxication of mammalian cells. J. Biol. Chem. **269:**20607–20612.
20. **Mock, M., E. Labruyère, P. Glaser, A. Danchin, and A. Ullmann.** 1988. Cloning and expression of the calmodulin-sensitive *Bacillus anthracis* adenylate cyclase in *Escherichia coli*. Gene **64:**277–284.
21. **Petosa, C., R. J. Collier, K. R. Klimple, S. H. Leppla, and R. Lidington.** 1997. Crystal structure of the anthrax toxin protective antigen. Nature **385:**933–938.
22. **Pezard, C., P. Berche, and M. Mock.** 1991. Contribution of individual toxin components to virulence of *Bacillus anthracis*. Infect. Immun. **59:**3472–3477.
23. **Pezard, C., E. Duflot, and M. Mock.** 1993. Construction of *Bacillus anthracis* mutant strains producing a single toxin component. J. Gen. Microbiol. **139:** 2459–2463.
24. **Ristroph, J. D., and B. E. Ivins.** 1983. Elaboration of *Bacillus anthracis* antigens in a new, defined culture medium. Infect. Immun. **39:**483–486.
25. **Shen, W. H., S. Y. Choe, D. Eisenberg, and R. J. Collier.** 1994. Participation of lysine 516 and phenylalanine 530 of diphtheria toxin in receptor recognition. J. Biol. Chem. **269:**29077–29084.
26. **Singh, Y., V. K. Chaudhary, and S. H. Leppla.** 1989. A deleted variant of *Bacillus anthracis* protective antigen is non-toxic and blocks anthrax toxin *in vivo*. J. Biol. Chem. **264:**19103–19107.
27. **Singh, Y., K. R. Klimpel, N. Arora, M. Sharma, and S. H. Leppla.** 1994. The chymotrypsin-sensitive site, FFD^{315}, in anthrax toxin protective antigen is required for translocation of lethal factor. J. Biol. Chem. **269:**29039–29046.
28. **Singh, Y., K. R. Klimpel, C. P. Quinn, V. K. Chaudhary, and S. H. Leppla.** 1991. The carboxyl-terminal end of protective antigen is required for receptor binding and anthrax toxin activity. J. Biol. Chem. **266:**15493–15497.
29. **Stanley, J. L., and H. Smith.** 1961. Purification of factor I and recognition of a third factor of anthrax toxin. J. Gen. Microbiol. **26:**49–66.
30. **Trieu-Cuot, P., C. Carlier, C. Poyart-Salmeron, and P. Courvalin.** 1990. A pair of mobilisable shuttle vectors conferring resistance to spectinomycin for molecular cloning in *Escherichia coli* and Gram positive bacteria. Nucleic Acids Res. **18:**4296.
31. **Vitale, G., R. Pellizzari, C. Recchi, G. Napolitani, M. Mock, and C. Montecucco.** 1998. Anthrax lethal factor cleaves the N-terminus of MAPKKs and induces tyrosine/threonine phosphorylation of MAPKs in cultured macrophages. Biochem. Biophys. Res. Commun. **248:**706–711.
32. **Vodkin, M. H., and S. H. Leppla.** 1983. Cloning of the protective antigen gene of *Bacillus anthracis*. Cell **34:**693–697.
33. **Wang, W.-M., R. Wattiez, F. Brossier, M. Mock, P. Falmagne, J.-M. Ruysschaert, and V. Cabiaux.** 1998. Use of a photoactivatable lipid to probe the topology of PA63 of *Bacillus anthracis* in lipid membranes. Eur. J. Biochem. **256:**179–183.

Editor: J. T. Barbieri